Geodynamic implications of ophiolitic chromitites in the La Cabaña ultramafic bodies, Central Chile

José María González-Jiménez

Departamento de Geología and Andean Geothermal Center of Excellence (CEGA), Facultad de Ciencias Físicas y Matemáticas, Universidad de Chile, Santiago, Chile

E-mail: jmgonzj@ing.uchile.cl

Fernando Barra

Departamento de Geología and Andean Geothermal Center of Excellence (CEGA), Facultad de Ciencias Físicas y Matemáticas, Universidad de Chile, Santiago, Chile

Richard J. Walker

Department of Geology, University of Maryland, College Park, MD 20742, USA

Martin Reich

Departamento de Geología and Andean Geothermal Center of Excellence (CEGA), Facultad de Ciencias Físicas y Matemáticas, Universidad de Chile, Santiago, Chile

Fernando Gervilla

Departamento de Mineralogía y Petrología and Instituto Andaluz de Ciencias de la Tierra (Universidad de Granada-CSIC), Fuentenueva s/n, Granada, Spain.

International Geology Review **56**, 1466-1483

Abstract

Chromitites hosted in two ultramafic bodies (Lavanderos and Centinela Bajo) from the Paleozoic metamorphic basement of the Chilean Coastal Cordillera were studied in terms of their chromite compositions, platinum-group element (PGE) abundances and Re-Os isotopic systematics. Primary chromite (Cr#=0.64-0.66; Mg#=48.71-51.81) is only preserved in some massive chromitites from the Centinela Bajo ultramafic body. This chemical fingerprint is similar to other high-Cr chromitites from ophiolite complexes, suggesting that they crystallised from arc-type melt similar to high-Mg island-arc tholeiites (IAT) and boninites in suprasubduction mantle. The chromitites display enrichment in IPGE (Os, Ir, Ru) over PPGE (Rh, Pt, Pd), with PGE concentrations between180 and 347 ppb, as is typical of chromitites hosted in the mantle of suprasubduction zone (SSZ) ophiolites. Laurite (RuS_2)-erlichmanite (OsS_2) phases are the most abundant inclusions of platinum-group minerals (PGM) in chromite, indicating crystallisation from S-undersaturated melts in the sub-arc mantle. The metamorphism associated with the emplacement of the ultramafic bodies in the La Cabaña has been determined to be ca. 300 Ma. Initial $^{187}Os/^{188}Os$ ratios for four chromitite samples, calculated for this age, range from 0.1248 to 0.1271. These isotopic compositions are well within the range of chromitites hosted in the mantle section of other Phanerozoic ophiolites. Collectively, these mineralogical and geochemical features are interpreted in terms of chromite crystallisation in dunite channels beneath a spreading center that opened a marginal basin above a suprasubduction zone. This implies that chromitite-bearing serpentinites in the metamorphic basement of the Coastal Cordillera are of oceanic-mantle origin and not portions of oceanic crust as previously suggested. We suggest that old subcontinental mantle underlying the hypothetical Chilenia microcontinent was unroofed and later altered during the opening of the marginal basin. This defined the geological framework in which the protoliths of the meta-igneous and meta-sedimentary rocks of the Eastern and Western Series of the Chilean Coastal Cordillera basement were formed.

Keywords: Chromite; ophiolite; marginal basin; Chile; Chilenia

1. Introduction

The Palaeozoic metamorphic basement of the Chilean south-central Coastal Cordillera contains scattered small bodies of serpentinised ultramafic rocks associated with a heterogeneous assemblage of meta-sedimentary and meta-volcanic rocks (Aguirre et al., 1972; Hervé, 1974, 1977; Godoy and Kato, 1990; Willner et al., 2005; Glodny et al., 2008). These ultramafic bodies and their host rocks have been suggested to be slices of a fossil oceanic lithosphere, which were accreted to the Pacific margin of Gondwana (Hervé et al., 1981; Forshythe, 1982; Glodny et al., 2005; Willner et al., 2005). The origin of the ultramafic rocks has been the subject of many studies and remains a hotly debated topic with two main hypotheses. An initial survey by Barra et al. (1998) of chromitite samples collected from streams draining the largest ultramafic bodies in the area of La Cabaña, about 60 km west of the city of Temuco (Fig. 1), revealed that these chromitites have an island arc signature. Additionally, Höfer et al. (2001) integrated the petrology and ages of deposition and metamorphism of the meta-sedimentary rocks with the mechanism of emplacement of the meta-volcanic and ultramafic rocks from La Cabaña, concluding that these rocks represent portions of oceanic lithosphere formed in a marginal basin developed behind an island arc, sited on the Paleo-Pacific margin of Gondwana. In contrast, Glodny et al. (2005) and Willner et al. (2005) based on studies of the northern part of the Coastal Cordillera (34°-36° S), have suggested that these are oceanic crustal rocks that were incorporated into the Coastal Cordillera by basal accretion.

These observations and contrasting models raise questions about the true origin of the chromitites and their host ultramafic rocks at La Cabaña, as well as their relationships to the surrounding meta-sedimentary and meta-volcanic rocks. In an attempt to bridge this gap we have examined the geochemistry of platinum-group elements (PGE), Re-Os isotopes and conducted *in situ* chemical analyses of chromite in chromitites from the La Cabaña ultramafic bodies. Our study contributes important data to the ongoing debate regarding interpretations of the origin and evolution of the metamorphic basement of the Chilean Coastal Cordillera, and provides new insights into the evolution of the Paleozoic eastern margin of the Gondwana supercontinent.

Geology of the chromitites

Geological overview of the metamorphic basement of central Chile

The La Cabaña ultramafic bodies (after Vergara, 1970) are situated near the town of Carahue in central Chile, approximately 60 km west of Temuco (Fig. 1). Geologically, they are part of the Palaeozoic metamorphic basement of the Chilean Coastal Cordillera, a paired metamorphic belt of Palaeozoic age that extends for more than 1,000 km along the south-central part of the Pacific coast of Chile. The westernmost unit of this metamorphic belt is known as the Western Series, whereas the easternmost belt is termed the Eastern Series. The rocks of these two units record distinct metamorphic grades: high-pressure/low-temperature (HP-LT) in the Western Series and low-pressure/high-temperature (LP-HT) in the Eastern Series (e.g., Aguirre et al., 1972; Godoy and Kato, 1990; Willner et al., 2005). The boundary between the two units is the sinistral NW-SE-striking Lanalhue Fault Zone (Glodny et al., 2008) in the south, whereas it is marked by a late reverse structure, the Pichilemu-Vichuquén Fault in the north (Willner et al., 2005).

The Western Series comprises meta-greywackes containing lenses of greenschists and blueschists and associated Fe, Mn-rich meta-sediments, meta-cherts and bodies of mafic-ultramafic rocks (upper mantle dunite, cumulate dunite-pyroxenites and gabbros), with some of them deformed and metamorphosed together with the surrounding host rocks (Aguirre et al., 1972; Hervé, 1977; Frutos and Alfaro, 1987; Barra et al., 1998; Höfer et al., 2001). Höfer et al. (2001) interpreted these rocks collectively as fragments of back-arc lithosphere. Although limited isotopic data exist for the metamorphic host rocks (e.g., Hervé et al., 2012), no isotopic data have been obtained so far for the mafic-ultramafic rocks.

The Eastern Series consists of alternating meta-sandstones and metapelites characterized by very low grades of metamorphism; these rocks are weakly deformed and mostly preserve the original bedding, except in the easternmost part of the belt where higher metamorphic grade have obliterated the primary fabric of the rocks (Hervé et al., 2012; Willner et al., 2000).

The Coastal Cordillera has been interpreted as either an accretionary complex (Hervé et al., 1981; Glodny et al., 2005, 2008; Willner, 2005; Willner et al., 2005), or

a backarc basin (Frutos and Alfaro, 1987; Rabbia et al., 1994; Hufmann and Massonne, 2000; Höfer et al., 2001) formed during the Late Carboniferous.

The La Cabaña Ultramafic Bodies

The La Cabaña ultramafic bodies consist of two small outcrops (Barra et al. 1998): the Centinela Alto (or Lavanderos) to the east and Centinela Bajo to the west (Fig. 2).

Lavanderos is a lens-like ultramafic body 200 × 35 m in size, trending N-S. It is hosted in Palaeozoic micaschists enclosing meta-volcanic rocks (Fig. 2; Vergara, 1970; Alfaro, 1980; Höfer et al. 2001). The body largely consists of antigorite, with accessory clinochlore and chromite mostly transformed to Fe^{2+}-rich porous chromite (Alfaro, 1980; Barra et al., 1998). Talc locally replaces both antigorite and chlorite. The antigoritite shows penetrative mylonitic foliation towards the boundaries of the body, which was most likely produced during its fault-controlled emplacement (Barra et al., 1998), or during greenschist-facies metamorphism (Höfer et al., 2001).

Centinela Bajo is a larger lobate body of 6 × 3 km in size that protrudes into the micaschists. The rocks are dunites made up of coarse-grained porphyroclastic olivine (1-2 mm) replaced by pseudomorphic (mesh texture) lizardite, with minor amounts of primary pyroxenes. The degree of alteration of the primary silicates may vary from 20 to 80% volume of the rock. The secondary silicates are accompanied by secondary chlorite and amphibole, and a late generation of chrysotile and carbonate veins crosscutting all the described mineralogy. Höfer et al. (2001) described an outcrop of meta-gabbros in contact with dunites in the northern part of the ultramafic body. However, in our field studies we did not find a continuous section from the mantle dunite to gabbros, owing to poor exposure in the rainforest. Despite the poor exposure Höfer et al. (2001) reported that the gabbros show clear evidence of metamorphism (uralitisation of clinopyroxene, secondary chlorite and minor zoisite and titanite), unlike the peridotites supposedly in contact with them. Detailed structural mapping reveals that shear zones filled by mylonite serpentinite surround and isolate blocks of undeformed serpentinized dunite; in the latter, mantle foliation (defined by trains of Cr-spinel in the porphyroclastic rocks) and random distributions of Cr-spinel grains are obliterated by the late mylonitic foliation near the contacts with the shear zones.

The foliations in the serpentinite rocks have a strike and dip identical to the foliation of the host schists (Fig. 2).

Chromitites

Chromitites have been reported in both ultramafic bodies at La Cabaña (Fig. 2 and 3; Barra et al., 1998; Höfer et al., 2001), although chromitites have only been observed *in situ* in Lavanderos (Fig. 3a-e). The Lavanderos chromitites are lenses and veins of a few centimetres thick of massive chromite (80% chromite) hosted in heavily serpentinised dunite (Fig. 3a-c). The contact between the massive chromitite and the host rock is sharp (Fig. 3c) but can locally grade to disseminated chromite ore through a zone of schlieren chromite (Fig. 3a-b). Frequently, late veins of chrysotile transgress the chromitite veins, disrupting their continuity (Fig. 3b-c). The metamorphic alteration that affected the rocks of the body has also completely transformed the magmatic chromite to secondary Fe^{2+}-rich porous chromite (Fig 4a; Barra et al. in review).

At Centinela Bajo, the poor exposure in the forest does not allow for direct observation of the chromitite bodies. We only identified a few blocks of massive chromitites on the slopes of the vegetation-covered hills (Fig. 2 and 3d-e). The features of these blocks, such as the massive texture of the ore, their irregular to angular shape and relatively large size, and their distribution along the drainage network led us to suspect the presence of hidden large chromitite bodies (Fig. 2; Höfer et al. 2001). The studied chromitite blocks consist of >90% former euhedral chromite grains, which are fractured and complexly zoned (Fig. 4b). The zoning consists of crystallographically-ordered rims (or patches) of Fe^{2+}-rich chromite (Gervilla et al., 2012) surrounding the unaltered (magmatic) cores. In the altered rims there are abundant inclusions of Cr-clinochlore, which may also fill one of the generations of fractures cutting the chromite grains. Cr-clinochlore is also the main constituent of the interstitial matrix between chromite grains (Barra et al. in review).

Methods

The compositions of major and minor elements in primary igneous cores of chromian spinels were obtained using a SX-100 CAMECA electron microprobe analyser (EMPA) at the Centro de Instrumentación Científica of the University of Granada (Spain), using the procedures described by Gervilla et al. (2012). In the former, calibration for chromite was performed using natural and synthetic standards: MgO for Mg, Fe_2O_3 for Fe, Al_2O_3 for Al, Cr_2O_3 for Cr, SiO_2 for Si, TiO_2 for Ti, $MnTiO_3$ for Mn, NiO_2 for Ni and $Pb_5(VO_4)_3Cl$ for V.

Six chromitite samples were analysed for bulk Platinum-Group Elements (PGE) abundances. The analyses were performed by Actlabs, Canada using nickel sulfide fire assay and instrumental neutron activation analysis (INAA) technique. Detection limits were 5 ppb for Ru and Pt, 2 ppb for Os and Pd, 0.2 ppb for Rh, 0.1 for Ir.

Whole-rock Re-Os isotopic analyses were performed on mineral separates of chromite from four selected chromitite samples. Chromite grains were analysed at the Isotope Geochemistry Laboratory, University of Maryland, USA, following the procedure described by Walker et al. (2002a). Briefly, about 0.5g of finely-ground coarse-grained chromite was introduced into a Pyrex^{TM} Carious tube with a 2:1 mixture of concentrated nitric and hydrochloric acids, and appropriate amounts of a mixed Re-Os spike. The tube was then sealed and heated at 270 °C for > 24 hours. Upon opening the tube, Os was separated by solvent extraction techniques (Cohen and Waters, 1996) and Re by standard column-chemistry procedure (Morgan and Walker, 1989). Osmium was further purified by microdistillation (Birck et al., 1997). Osmium isotopic ratios wre determined using the UMd *VG Sector* 54 thermal ionisation mass-spectrometry (TIMS) using Faraday cups, whereas Re abundances were analysed using a Cetac Aridus nebuliser coupled to a Nu Plasma multi-collector inductively-coupled mass spectrometer (MC-ICP-MS). External precision for $^{187}Os/^{188}Os$, and Os and Re concentrations for the quantities measured was better than 0.1%, 0.2% and 2% respectively. Procedure blanks averaged 0.8 picograms for Os and 1.2 picograms for Re. Blank corrections for Os were negligible (<0.1%). Blank corrections for Re comprised as much as 1% for some samples. Initial $^{187}Os/^{188}Os$ ratios are calculated as per Shirey and Walker et al. (1998).

Results

227 *Chemistry of primary chromite*

228 As the La Cabaña chromitites are variably altered, interpretations of their
229 petrogenesis in terms of primary magmatic processes in the mantle require the
230 analysis of the unaltered cores of chromite grains. Primary cores were only preserved
231 in the massive chromitite of Centinela Bajo (Fig 4b and 5a-d; Barra et al., 1998). The
232 assumption of an igneous origin for these cores is supported by EMPA analyses
233 showing that they contain very low Fe_2O_3 (< 2.60 wt.%; *i.e.*, [Fe^{3+}# =
234 $Fe^{3+}/(Fe^{3+}+Al^{3+}+Cr^{3+})$] < 0.03), high MgO (> 12.09 wt.%), and low TiO_2 (< 0.23
235 wt.%), values that are typical for primary chromite from mantle-hosted ophiolitic
236 chromitites (Fig. 5a-b; Table 1).

237 The primary chromite of the Centinela Bajo chromitites is highly homogeneous in
238 terms of Cr# [Cr/(Cr+Al) atomic ratio] and Mg# [Mg/Mg+Fe^{2+} atomic ratio] (Fig.
239 5c). Thus, the Cr# values range between 0.64 and 0.66, which correspond to 48.71-
240 51.81 wt% Cr_2O_3 and 17.33-18.52 wt% Al_2O_3, whereas the Mg# varies from 0.58 to
241 0.67. These Cr# and Mg# values overlap with the compositional field of high-Cr
242 podiform ophiolitic chromitite (Fig. 5a-c). The contents of MnO, V_2O_3 and ZnO are
243 lower than 0.48 wt%, 0.29 wt% and 0.20 wt%, respectively.

244 *Platinum-group elements (PGE)*

245 The La Cabaña chromitites have relatively low PGE concentrations, with total
246 PGE contents from 180 to 347 ppb for each of the samples (Table 2), with slightly
247 higher concentrations in samples from Centinela Bajo (294-347 ppb; mean 320 ppb)
248 relative to those from Lavanderos (180-235; mean 213 ppb). Figure 6 shows the
249 chondrite-normalised distribution pattern of the La Cabaña chromitites compared with
250 chromitites hosted in the mantle section of other ophiolites, and from other
251 geodynamic settings. The general compositional trend of the La Cabaña chromitites
252 fits very well with the distribution of the PGEs shown by other Type I chromitites
253 (González-Jiménez et al., 2013c) that are hosted in the mantle sequence of ophiolite
254 complexes and show an enrichment in the IPGE (Os, Ir and Ru =305-346.9 ppb)
255 relative to PPGE (Rh, Pt and Pd=13.9-42.9 ppb).

256 The La Cabaña chromitites exhibit steep positive patterns from Os to Ru (with Ir
257 positive anomalies to Os and Ru in the samples CAB-7B and PODOB), followed by

steep negative slopes from Rh to Pd (with Pd positive anomalies in the samples CAB-7B, LAC-2). This distribution of the PGEs in the La Cabaña chromitites also overlaps the fields of other Latin American chromitites hosted in the mantle sections of supra-subduction zone (SSZ) ophiolites (Fig. 6), such as the "unmetamorphosed" high-Cr chromitites in Sagua de Tánamo, eastern Cuba (González-Jiménez et al., 2011) and the "metamorphosed" high-Al chromitites of Tehuitzingo, SW Mexico (Proenza et al., 2004). These have been interpreted as crystallised from melts with back-arc basin basalt (BABB) affinity. In contrast, the La Cabaña chromitites have lesser amounts of IPGE and a less pronounced negative segment from IPGE to PPGE than the chromitites (high-Cr) of the Vizcaino Peninsula, Mexico (Vatin-Perignon et al., 2000) and Santa Elena in the Dominican Republic (high-Cr and high-Al; Fig. 6b; Zaccarini et al., 2011). These chromitites are interpreted to have crystallised in equilibrium with melts of boninitic affinity, generated by hydrous melting in suprasubduction environments. Finally, the La Cabaña chromitites are significantly different from the high-Al chromitites of the Pampean Ranges, Argentina, in which metamorphism has disturbed the original distribution of PGEs (Fig. 6b; Proenza et al., 2008).

The abundances of IPGE in the La Cabaña chromitites were controlled by abundant inclusions of Os-Ir-Ru alloys, laurite (RuS_2)-erlichmanite (OsS_2), irarsite (IrAsS), and minor omeiite ($OsAs_2$), and Ru-Ni alloys (Galdames et al., 2011). The PPGE-rich assemblage mainly includes Rh-rich minerals such as hollingworthite (RhAsS) and an unidentified antimonide (Rh-Cu-Sb). Laurite-erlichmanite is found as inclusions in the cores of chromite grains but is more commonly replaced by Os-Ir-Ru alloys in pores of Fe^{2+}-rich chromite, suggesting its desulfurisation under reducing conditions. This process could be also responsible for the formation of Ru-Ni alloys after breakdown of Ru-bearing Ni-rich sulfides. In contrast, irarsite, omeeite and the unnamed Rh-Cu antimonide are most likely associated with oxidising fluids, which supplied As and Sb to the system, and redistributed the PGE. Abundant secondary inclusions of Ni-rich S-poor sulfides (heazlewoodite and gersdorfite) and Ni-arsenides accompany these PGMs in the alteration rims of chromite.

Whole-rock Re-Os isotopes

Total Re in La Cabaña chromitites is very low (<0.35 ppb), with the exception of sample CEN-07, which shows a slightly higher content (2.2 ppb). Osmium concentrations vary from 38–202 ppb (Table 3). Measured $^{187}Os/^{188}Os$ ratios of chromite separates from three chromitite blocks of Centinela Bajo vary from 0.1252 to 0.1271, and a chromite separate from one chromitite pod from Lavanderos has a ratio of 0.1268 (Table 3). The $^{187}Os/^{188}Os$ for all four chromite averages of 0.12652 ± 0.0008 (2σ). Estimates for the present $^{187}Os/^{188}Os$ ratio of the bulk oceanic mantle today ranges from a low of ~ 0.125, based on the average of abyssal peridotites (e.g., Snow and Reisberg, 1995; Liu et al., 2009), to a high of ~ 0.128, based on averages for chromitites and peridotites of Phanerozoic ophiolites extrapolated to the present (e.g., Walker et al., 2002b). Thus, ratios for all of our chromitite samples fall well within the range of estimates for the modern oceanic mantle.

Initial $^{187}Os/^{188}Os$ ratios have been calculated for 300 Ma, which is the estimated age of emplacement of the peridotites onto the continental crust inferred from the age of metamorphism of the meta-sedimentary rocks hosting the peridotites (Höfer et al., 2001; Willner et al., 2005). These ratios are almost identical to the measured ratios because of the very low Re/Os ratios of the chromitites. At La Cabaña, the initial $^{187}Os/^{188}Os$ ratios span from 0.1248 to 0.1271, with an average of 0.1264 ± 0.0011 (2σ) (Fig. 7). Although the total number of samples analysed for Os isotopes is too small to be statistically robust, there appear to be no major differences in Os isotopic compositions between chromitites of Centinela Bajo and Lavanderos.

Discussion

Parental melts of the chromitites

The composition of primary magmatic cores of chromite from Centinela Bajo chromitites with high Cr, and low Fe_2O_3 and TiO_2 contents is typical of chromite from chromitites hosted in the upper mantle sequence of ophiolite complexes (Fig. 5a-b). In the Al_2O_3 versus TiO_2 diagram defined by Kamenetsky et al (2001) for chromites hosted in lavas of different geotectonic settings (Fig. 5d), some of these cores fall within the field of MORB, but most plot close to spinels with high Ti from basalts of modern back-arc basins; another set of data with lower TiO_2 plots out of these fields. This is a common feature of many mantle-hosted chromitites worldwide (e.g., Pagé

and Barnes, 2009; Zaccarini et al., 2011; Escayola et al. 2012), which may reflect the increase of TiO_2 produced in melts crystallising chromitite as they migrate through the SSZ mantle while reacting with peridotite wall-rock (Graham et al., 1996; Zaccarini et al., 2011; González-Jiménez et al., 2011, 2013c).

Experimental and empirical studies show that the contents of Al_2O_3, TiO_2, FeO and MgO in chromite reflect those of the melt from which the chromite has crystallised (Maurel and Maurel, 1982; Wasylenki et al., 2003; Kamenetsky et al. 2001; Rollinson, 2008; Pagé and Barnes, 2009). Considering that our chromites are high-Cr (Fig. 5b-d) and low-Ti, similar to chromite from low-Ti high-Cr arc-lavas of Kamenetsky et al. (2001), we have estimated the Al_2O_3 and TiO_2 contents of the melt(s) in equilibrium with our chromite using the revised equations defined by Zaccarini et al. (2011) for those chromites (eqs. 1 and 2):

$$ln\ [wt\%\ Al_2O_{3\ (melt)}] = 5.2253 \times ln\ [Al_2O_{3\ (spinel)}] - 1.1232\ (R^2=0.9723) \quad \text{(eq. 1)}$$

$$ln\ [wt\%\ TiO_{2\ (melt)}] = 1.0897\ ln[wt\%\ TiO_{2\ (spinel)}] + 0.0892 \quad \text{(eq. 2)}$$

The FeO/MgO ratios of the melts in equilibrium with Centinela Bajo chromites were estimated using the following empirical expression (Maurel and Maurel, 1982; equation 3):

$$ln(FeO/MgO)_{spinel} = 0.47 - 1.07Al\#_{spinel} + 0.64Fe^{3+}\ \#_{spinel} + ln\ (FeO/MgO)_{melt} \quad \text{(eq. 3)}$$

where FeO and MgO in wt%, $Al\# = Al/(Cr+Al+Fe^{3+})$ and $Fe^{3+}\# = Fe^{3+}/(Cr+Al+Fe^{3+})$.

These calculations suggest that the melts that have precipitated the chromite of the Centinela Bajo chromitites contained from 13.7 to 14.2 wt% Al_2O_3, and from 0.22 to 0.34 wt% TiO_2, with FeO/MgO varying between 0.8 and 1.2. The Al_2O_3 contents of the parental melt in equilibrium with the igneous chromite of the Centinela Bajo are similar to the melts that precipitated the high-Cr chromites in boninite lavas at Bonin Island in Japan (10.6-14.4 wt% Al_2O_3; Hicky and Frey, 1982; Crawford et al., 1989), but also overlap those of high-Mg island-arc tholeiites (IAT) (11.4-16.4 wt% Al_2O_3; Augé, 1987).

Similar arc-type melts but with lower Al_2O_3, TiO_2 and FeO/MgO have been suggested to be responsible for the formation of high-Cr chromitites in the mantle

section of many SSZ ophiolites. Examples include Kempirsai in Kazakhstan (Melcher et al., 1997), Oman (Rollinson, 2008), Muğla in Turkey (Uysal et al., 2009), Rutland Island in the Bay of Bengal (Ghosh et al., 2009), Santa Elena in Costa Rica (Zaccarini et al., 2011), and Mayarí-Cristal, in eastern Cuba (Proenza et al., 1999; González-Jiménez et al., 2011). These chromitites were interpreted to have crystallised near the Moho Transition Zone (MTZ) of oceanic lithosphere overlying a subduction zone in either a fore-arc or back-arc basin.

On the other hand, the La Cabaña chromitites show the typical chondrite-normalised PGE patterns of ophiolitic chromitites characterised by the enrichment in IPGE (i.e., Os, Ir and Ru), which differ significantly from chromitites found in layered mafic intrusions and Ural/Alaskan complexes (Fig. 6a). The inclusions of primary Os-rich PGMs like laurite, as a mineralogical expression of the abundances of IPGEs, indicate the sulfur-undersaturated nature of the melts that crystallised the chromitites (Garuti et al., 1999; Brenan and Andrews, 2001; Andrews and Brenan, 2002; Bockrath et al., 2004). Basaltic melts with low enough fS_2 to precipitate Os-rich PGMs are produced during the partial melting of depleted peridotites (Jugo, 2009), or secondarily by the reaction of IAT melts with mantle peridotite at increasing melt/rock ratio during the formation of chromitites, in a SSZ mantle (Zhou et al., 1998; Büch et al., 2002; Shi et al. 2007; Marchesi et al., 2011).

Tectonic setting of the La Cabaña ultramafic bodies

According to Prichard et al. (2008), chromitites with appreciable amounts (~100 ppb) of total PGEs are precipitated only from melts that have been extracted after ≥20% partial melting of mantle sources. The fact that at La Cabaña the average PGE content of chromtites is around 250 ppb suggests that the melts were derived from a mantle source that had experienced degrees of partial melting above 20%. The primary olivine preserved in the dunites at Centinela have Mg# = 0.90-0.92 and Ni contents (0.16-0.45 wt%), similar to the olivine in the ultra-depleted peridotites of the mantle section of ophiolites of Eastern Cuba (Fig. 8). This leads us to suggest that the dunites hosting the chromitites at Centinela Bajo are residues resulting from high degrees of partial melting.

In the ophiolite environment, peridotites that have undergone multiple episodes of melt extraction until nearly barren in their major- and minor-elements signatures are common in the mantle beneath arcs developed above suprasubduction zones. In these settings, dehydration of the subducting slab may release a large volume of volatiles contributing to a decrease in the melting temperature, thus favouring the release of PGEs from their host peridotitic mantle at lower degrees of partial melting than relatively fertile, "dry" and less oxidised settings such as MOR (Jugo, 2009). Chromitites that have crystallised in a MOR setting are significantly more depleted in PGEs than those from the La Cabaña (Leblanc and Nicolas, 1992; Zhou et al., 1996, 1998; Proenza et al. 1999; Prichard et al, 2008; Uysal et al., 2009; González-Jiménez et al. 2013c).

The similar geochemistry of the studied chromitites to "mantle hosted" chromitites from SSZ ophiolites provide the first evidence that the La Cabaña ultramafic bodies are portions of an oceanic mantle overlying a suprasubduction zone. The formation of chromitites in the suprasubduction zone environment is commonly associated with the crystallisation of basaltic melts at their site of extraction during the opening of marginal basins in either fore-arc or back-arc basins (Roberts, 1998; Leblanc and Nicolas, 1992; Malpas, 1997; Melcher et al., 1997; Proenza et al., 1999; Rollinson, 2005, 2008; Gervilla et al., 2005; González-Jiménez et al., 2013c; Robinson and Adetunji, 2013). This is consistent with the fact that the widespread meta-volcanic rocks and metabasites in the Western Series show E-MORB signatures (Rabbia et al., 1994; Hufmann and Massone, 2000), suggesting that these rocks crystallised from basaltic melts derived from an upwelling mantle beneath a spreading centre. During the formation and evolution of the marginal basin above a suprasubduction zone, the extraction of melts from the mantle takes place preferentially through dunite conduits sited beneath the axis of the spreading ridge. Numerical modelling (Braun and Kelemen, 2002) shows that in these settings the dunite conduits form an interconnected network of channels filled with basaltic melts that might be extracted from different mantle sources. Where two or more melt-filled conduits intersect, batches of melt with different degrees of fractionation (i.e., different $a\mathrm{SiO_2}$) may mix to produce hybrid melts saturated with chromite, and thus, are capable of crystallising sizeable chromitite bodies (González-Jiménez et al., 2013c).

411 Under the proposed scenario, the upwelling arc-type melts might become saturated
412 in chromite precipitating chromitites prior to their emplacement at crustal levels as
413 mafic rocks or extruded lavas. A similar interpretation has been proposed for other
414 ophiolites (Leblanc, 1986; Graham et al., 1996; González-Jiménez et al., 2011), and
415 firmly demonstrated by analysis of minor- and trace-element in chromite from a suite
416 of mantle and crustal rocks of Oman (Dare et al., 2009) and Thetford Mines in
417 Canada (Pagé and Barnes, 2009). Thus, our observations and data provide significant
418 evidence against previous interpretations that the metabasites and their associated
419 ultramafic rocks (i.e., serpentinites and peridotites) found in the metamorphic
420 basement of the Coastal Cordillera represent the segments of *the upper part of an*
421 *oceanic crust* (Willner, 2005). In contrast, we propose that these rocks correspond to
422 different fragments of oceanic lithosphere (including mantle and overlying crust) that
423 originally formed in a marginal basin developed above a suprasubduction zone. Most
424 likely these portions of upper mantle were later incorporated into the continental crust
425 by basal accretion within the accretion prism represented by the metamorphic rocks of
426 the Coastal Cordillera.

427 *Interpretation of the Re-Os isotopic data*

428 As is typical of ophiolitic chromitites worldwide, the four La Cabaña
429 chromites are characterised by very low $^{187}Re/^{188}Os$, hence, calculated initial ratios
430 are not very sensitive to the formation age. Here, we have used the estimated age of
431 the host rocks metamorphism (ca. 300 Ma) to calculate the initial $^{187}Os/^{188}Os$ ratios.
432 However, it is reasonable to think that this is a minimum age because the chromitites
433 and PGE inclusions could have formed several million years before their
434 emplacement onto the continental crust (e.g., González-Jiménez et al., 2013b). Of
435 note, the initial $^{187}Os/^{188}Os$ ratios of the la Cabaña chromites fit well with the average
436 evolution curve for chromitites of SSZ ophiolites worldwide (Fig. 7; Walker et al.,
437 2002b).

438 The initial $^{187}Os/^{188}Os$ ratios of La Cabaña chromites, however, vary little
439 compared with much larger variations noted for most other chromitites from
440 Phanerozoic ophiolites (Fig. 7a). Büchl et al. (2000) also observed small variations of
441 Os in chromitite pods hosted in the mantle section of the Troodos ophiolite. In these
442 chromitites the range of variation of $^{187}Os/^{188}Os$ ratios of the chromite separates

(0.1265-0.1301) is much lower than those of the associated peridotites (0.1235-0.1546). These authors suggest that during the formation of the chromitites under an open-system, potentially with significant input of numerous melts with variable composition, the mixing process involved in the formation of chromitites tend to homogenize the Os signatures. This is surprising, as the Os isotopic compositions are likely governed by the presence of discrete inclusions of PGM and BMS formed from melt/fluids with diverse magmatic and post-magmatic contributions (Fig. 7; Malitch et al., 2003; Malitch 2004; Ahmed et al., 2006; Shi et al., 2007; Marchesi et al., 2011; González-Jiménez et al., 2012a,b, 2013a,b).

Additionally, recent work on ophiolite chromitite often contain several populations of PGM and BMS with different Os-isotope signatures at the sub-grain scale (e.g., Marchesi et al., 2011; González-Jiménez et al., 2012a,b, 2013a). The analysis *in-situ* using LA-MC-ICPMS of large datasets of individual PGMs and BMS from chromitites and host peridotites in the Ojen massif in Spain suggest that the formation of these chromitites, which involved partial melting, melt transport/pooling and melt–rock reactions, did not erase the original $^{187}Os/^{188}Os$ heterogeneity of the peridotite source (Gonzalez-Jiménez et al., 2012b). Indeed, the results of this study highlights the complexity of the mechanism of formation of the chromitites in ophiolites, which may require the fractional extraction and/or steeped pooling of melts for the preservation of the Os signatures during the mingling process necessary to crystalise chromite (González-Jiménez et al., 2012b).

A new geodynamic framework for the mafic-ultramafic rocks of the Chilean Coastal Cordillera

The structure of the present western margin of the South American continent is seen as the result of the amalgamation of several tectonostratigraphic terranes to the southern Andean margin during the Palaeozoic (Ramos et al., 1986; Bahlburgh et al., 1994; Ramos 2008, 2009; Bahlburgh et al., 2009). During the early to middle Devonian the hypothetical exotic terrane known as Chilenia (Ramos et al., 1984; Ramos and Basei, 1997; Keppie and Ramos, 1999) was separated from Laurentia and later accreted to the proto-Andean margin in the south-central part of Chile (Ramos et al., 1986; Davis et al., 2000; Ramos, 2008). Rb-Sr and K-Ar ages suggest that the continental crust of the Chilenia micro-continent was later intruded by the Southern

475 Coastal Batholith ca. 295-307 Ma ago (Hervé et al., 1988; Lucassen et al., 2004;
476 Glodny et al., 2008). The geochemical and isotopic studies indicate that the parental
477 melts of these intrusive rocks were derived from a portion of sub-arc mantle overlying
478 a suprasubduction zone (Lucassen et al., 2004). These observations lead us to suggest
479 that this section of the paleo-margin of Gondwana has remained as a passive margin
480 until the early Late Carboniferous when a paleo-subduction zone was initiated (Fig.
481 9). This interpretation is consistent with previous hypotheses that the paleomargin of
482 Gondwana was a passive margin from Ordovician to Early Carboniferous time (Hervé
483 et al., 1987; Bahlaburg and Hervé, 1997; Augustsson and Balhburg, 2003). The
484 formation of sedimentary rocks that now constitute the Western Series is related to the
485 erosion of Chilenia, as is indicated by the U-Pb ages of detrital zircons in these units
486 (Hervé et al., 2012).

487 Rapialini and Vilas (1991) suggested that between the Late Carboniferous and the
488 Early Permian, the vector of subduction of the Proto-Pacific changed to a northward
489 oblique direction, which resulted in the rotation of several continental blocks with
490 strike-slip displacement parallel to the western continental margin of South America.
491 This interpretation, based on paleomagnetic studies is consistent with the fact that the
492 Lanalhue Faut zone acted, in its initial stages of development, as a ductile
493 deformation zone with divergent character (Glodny et al., 2008). We suggest that this
494 change of the tectonic regime, which very likely also increased the angle of the
495 subducting slab coupled with the associated rollback of the subducting plate,
496 enhanced the break-up of a portion of Chilenia by opening of a pull-apart basin (Fig.
497 9).

498 The emplacement of the La Cabaña peridotites into the continental crust is poorly
499 constrained at 282 ± 6 Ma , based on K-Ar dating of fuchsite, whereas granitoids
500 intruded the continental crust of Chilenia ca. 295-307 Ma. This suggest that this
501 marginal basin was active for a very short period (~10 Ma) and that peridotites
502 representative of ancient SCLM beneath Chilenia could be altered (i.e., oceanised),
503 and later served as the basement for the accumulation of oceanic basalts and
504 sediments, similar to that observed in other oceanic basins (Tsuru et al. 2000; Shi et
505 al., 2007; 2013; Griffin et al., 2009; O'Reilly et al., 2009; Tang et al., 2013). This
506 marginal basin must have been limited to the east by a fragment of the former

Chilenia terrain (Fig. 9). Additional evidence for the formation of this marginal basin is provided by the geochemistry of the chromitites presented here, and the E-MORB signature of the metabasites widespread through the Western Series (Díaz et al., 1988; Vivallo et al., 1988; Rabbia et al., 1994; Hufmann and Massone, 2000). This interpretation is also consistent with the presence of several Besshi-type massive sulfide deposits interpreted as formed in a proximal setting in a marginal basin (Alfaro and Collao, 1990; Schira et al., 1990). In this new model, the protolithic sedimentary rocks of the Western Series resulted from erosion and later sedimentation within the marine basin of Carboniferous granitic plutons and possibly some parts of the previously-formed Eastern Series (Fig. 9).

A compressive regime can be related with the Early- to Mid-Permian San Rafael orogeny, during which the previously separated fragment of Chilenia docked with the Chilean paleo-Pacific margin as described by Mpodozi and Kay (1990, 1992) for the northern part of Chile (28°-31°S), producing the Early Permian metamorphism preserved in the rocks of both Western and Eastern Series (Höfer et al., 2001; Glodny et al., 2008). We currently lack evidence for this fragment of Chilenia, which may have been lost by tectonic erosion associated with subduction and/or its assimilation by Triassic granitic magmatism now preserved at the coast near the city of Concepción (Lucassen et al., 2004).

Conclusions

(1) The geochemistry signature of the La Cabaña chromitites suggests that they precipitated from arc-type melts originated within a suprasubduction zone environment. This new interpretation rules out previous models that have suggested that the mafic and ultramafic rocks of the Coastal Cordillera were formed in an abyssal setting.

(2) The initial $^{187}Os/^{188}Os$ ratios for four chromitite samples, calculated for the estimated age of emplacement, range from 0.1248 to 0.1271. These isotopic compositions are within the worldwide range of reported Re-Os data for chromitites from other Phanerozoic ophiolites.

(3) The formation of the chromitites was associated with the formation and evolution of a marginal basin above the supraduction zone. However, unlike most chromitites reported worldwide, this basin did not develop behind an

island arc but in a fore-arc setting. Available regional data suggest that they originated in a pull-apart basin that separated a portion of the Chilenia microcontinent. The opening of this marginal basin was associated with the change in the direction of subduction in the paleo-Pacific subduction zone, and involved the "oceanisation" of the old subcontinental lithospheric mantle.

Acknowledgements

The authors are grateful to the Editor, XXX for editorial handling, and to XXX referees for their constructive criticisms, which greatly improved our manuscript. We thank Prof. William L. Griffin, Macquarie University, Australia for his review of an earlier version of this manuscript. This research was funded by FONDECYT project #1110345 and the project CGL2010-15171 funded by the Spanish Ministry of Education and Science.

Figure captions

Figure 1. Geological sketch map of the Coastal Cordillera of south-central Chile with the location of the La Cabaña área (modified from SERNAGEOMIN, 2003)

Figure 2. Simplified geological map of the La Cabaña area (modified from Höfer et al., 2001) showing the location of chromitite bodies observed *in situ* and collected from the rainforest drainage network. Legend is inset in the figures.

Figure 3. Photographs showing morphologies and structures of the studied chromitites in the La Cabaña ultramafic bodies. (a), (b) and (c) are chromitites observed *in situ* at Lavanderos whereas (d) and (e) are boulders of chromitite collected from the rainforest drainage network. In photographs (b) and (c) late chrysotile (Ctl) veins in disrupt the chromitite.

Figure 4. Back-scattered electron (BSE) images showing textures of chromitites of the La Cabaña area. (a) chromite grain completely transformed to secondary porous chromite at Lavanderos, (b) partly altered chromite with porous chromite rim and homogenous unaltered core at Centinela Bajo. We use the definition of porous chromite and partly altered chromite microstructures as defined Gervilla et al. (2012).

Figure 5. Chemistry of primary chromite of the Centinela Bajo chromitite as comparison with chromian spinel of various tectonic settings in terms of (a) Al-Cr-Fe^{3+} compositions, (b) TiO_2 versus Cr_2O_3. (c) Cr# [Cr/(Cr+Al)] versus Mg# [Mg/(Mg+Fe)]. (d) TiO_2 versus Al_2O_3. Data sources for chromian spinel of different tectonic settings taken from Kamenetsky et al. (2001) and Proenza et al. (2007).

Figure 6. C1-chondrite (Naldrett and Duke, 1980) normalized patterns of the La Cabaña chromitite and comparison with the chromitites hosted in the ophiolitic mantle (Proenza et al., 2007 and references therein) and in Alaskan-type complexes (Garuti et al., 2003, 2005) of the Urals and Bushveld (UG2) Layered Complex (Naldrett et al., 2011). Other selected chromitites (with high-Cr and high-Al chromite) of Latin America have been included for comparison: Vizcaino, Baja California Sur, Mexico (Vatin-Perigon et al., 2000); Tehuitzingo, Acatlan Complex, Mexico (Proenza et al., 2004); Pampean Ranges, Argentina (Escayola et al., 2004); Santa Elena, Costa Rica (Zaccarini et al., 2011); Sagua de Tánamo, Mayarí-Baracoa ophiolite, Cuba (González-Jiménez et al., 2011).

Figure 7. Initial $^{187}Os/^{188}Os$ versus presumed age (Ga) of ophiolite formation for the La Cabaña chromitites and other chromitites hosted in the mantle sections of Phanerozoic SSZ ophiolites. Here the term "age of ophiolite formation" is considered as either timing of the incorporation of the peridotite substrate into an "oceanic" column, with an overlay of basaltic and gabbroic crust and sediments, or the time when the crust-mantle sequence was emplaced onto the continental crust for preservation. The gray line represents the evolution trajectory for the primitive upper mantle (PUM) as reported by Meisel et al. (2001) whereas black one corresponds to estimates for chromitites worldwide (Walker et al., 2002b). The plot for whole-rock and chromite separates includes data reported by Walker et al. (2002b) for chromitites worldwide ophiolites as well as data for Albania (Kocks et al., 2007); Kraubath. Austria (Melcher and Meisel, 2004); Shetland, Scotland (Walker et al., 2002b; O'Driscoll et al. 2012); Mayarí-Baracoa, Cuba (Gervilla et al., 2005; Frei et al., 2006), Mugla, Turkey (Uysal et al., 2009); Sartohay, China (Shi et al., 2012). The data source for *in-situ* PGM: Eastern Desert, Egypt (Ahmed et al., 2006), Dobromirtsi, Bulgaria (González-Jiménez et al., 2013d), Kraubath, Austria (Malitch, 2004), Loma Baya (González-Jiménez et al., 2013b), Luobusa and Donqiao, Tibet (Shi et al., 2007), Mayarí and Sagua de Tánamo, Cuba (Marchesi et al., 2011; González-Jiménez et al., 2012a), Oman (Ahmed et al., 2006), Ojén (González-Jiménez et al., 2013a).

Figure 8. Ni versus Mg in olivine relics in dunites of Centinela Bajo; these are very similar to those in ultra-depleted peridotites of the Cuban ophiolites (Proenza et al., 1999).

Figure 9. New geodynamic model proposed for the evolution of the Chilean Coastal Cordillera.

Tables

Table 1. Selected analyses of unaltered chromite cores of Centinela Bajo chromitites

Table 2. Platinum-group elements of chromitite samples from the La Cabaña ultramafic bodies.

Table 3. Re and Os isotopes and abundances of selected chromite samples from the La Cabaña ultramafic bodies.

Table 4. Representative compositions of olivine relics in dunites from the Centinela Bajo ultramafic body.

References

Aguirre, L., Hervé, F., Godoy, E., 1972. Distribution of metamorphic facies in Chile, an outline. *Kristalinikum*, **9**, 7–19.

Ahmed, A.H., Hanghøj, K., Kelemen, P.B., Hart, S.R., Arai, S., 2006. Osmium isotope systematics of the Proterozoic and Phanerozoic ophiolitic chromitites: in situ ion probe analysis of primary Os-rich PGM. Earth and Planetary Science Letters 245, 777–791.

Alfaro, G. 1980. Antecedentes preliminares sobre la composición y génesis de las cromitas de La Cabaña (Cautín). Revista Geológica de Chile, 11, 29-41.

Alfaro, G., Collao, S., 1990. Massive Sulfides in the Greenstone Belt of South-Central Chile – An Overview. In: FONTBOTË, L., AMSTUTZ, G. C., CARDOZO, M., CEDILLO, E. & FRUTOS, J. (eds) Stratabound Ore Deposits in the Andes. Springer, Berlin, 199-208

Andrews, D.R.A., Brenan, J.M., 2002. Phase-equilibrium constraints on the magmatic origin of laurite and Os–Ir alloy. Canadian Mineralogist 40, 1705–1716.

Augé, T., 1987. Chromite deposits in the northwestern Oman ophiolite: mineralogical constraints. Mineralium Deposita 22, 1–10.

Augustsson, C., Bahlburg, H., 2003. Active or passive continental margin? Geochemical and Nd isotope constraints of metasediments in the backstop of a pre-Andean accretionary wedge in southernmost Chile (46°30′–48°30′S). In: MCCANN, T. & SAINTOT, A. (eds) Tracing Tectonic Deformation Using the Sedimentary Record. Geological Society, London, Special Publications, 208, 253–268.

Bahlburg, H., Hervé, F., 1997. Geodynamic evolution and tectonostratigraphic terranes of northwestern Argentina and northern Chile. GSA Bulletin, 109, 869–884.

Bahlburg, H., Moya, C., Zeil, W., 1994. Geodynamic evolution of the early Palaeozoic continental margin of Gondwana in the Southern Central Andes of Northwestern Argentina and Northern Chile. In: REUTTER, K.-J., SCHEUBER, E. & WIGGER, P. (eds) Tectonics of the Southern Central Andes. Springer, Berlin, 293–302.

657 Bahlburg, H., Vervoort, J.D., Du frane, S.A., Bock, B., Augustsson, C., Reimann, C. 2009.
658 Timing of crust formation and recycling in accretionary orogens: Insights learned from the
659 western margin of South America. Earth-Science Reviews, 97, 215-241.

660 Barra F., Gervilla, F., Hernández, E., Reich, M. & Padrón-Navarta J. A. (in review) Altered
661 chromian spinels from La Cabaña peridotite, south central Chile: Considerations on the
662 formation of ferritchromite.

663 Barra, F., Rabbia, O.M., Alfaro, G., Miller, H., Hofer, C., Kraus, S. 1998. Serpentinitas y
664 cromititas de La Cabaña, Cordillera de la Costa, Chile central. Revista Geológica de Chile,
665 25, 29-44.

666 Birck, J.-L., Roy-Barman, M., Capmas, F., 1997. Re–Os isotopic measurements at the
667 femtomole level in natural samples. Geostandards Newsletter 20, 9–27.

668 Bockrath, C., Ballhaus, C., Holzheid, A., 2004. Stabilities of laurite RuS_2 and monosulphide
669 liquid solution at magmatic temperature. Chemical Geology 208,265–271.

670 Braun, M.G., Kelemen, P.B., 2002. Dunite distribution in the Oman Ophiolite: implications
671 formelt flux through porous dunite conduits. Geochemistry, Geophysics, Geosystems 3
672 (11), 8603. http://dx.doi.org/10.1029/2001GC000289.

673 Brenan, J.M., Andrews, D., 2001. High-temperature stability of Laurite and Ru–Os–Ir alloy
674 and their role in PGE fractionation in mafic magmas. The Canadian Mineralogist 39, 341–
675 360.

676 Büchl, A., Brügmann, G., Batanova, V.G., Münker, C., Hofmann, A.W., 2002. Melt
677 percolation monitored by Os isotopes and HSE abundances: a case study from the mantle
678 section of the Troodos Ophiolite. Earth and Planetary Science Letters 204, 385–402.

679 Cohen, A. S., Waters F. G., 1996. Separation of osmium from geological materials by solvent
680 extraction for analysis by TIMS. Analytica Chimica Acta 332, 269–275.

681 Crawford, A.J., Fallon, T.J., Green, D.H., 1989. Classification, Petrogenesis and Tectonic
682 Setting of Boninites. In: Crawford, A.J. (Ed.), Unwin and Hyman, London, pp. 2–44

683 Dahlquist, J.A., Rapela, C.W., Pankhurst, R.J., Fanning, C.M., Vervoort, J.D., Hart, G.,
684 Baldo, E.G., Murra, J.A., Alasino, P.H., Colombo, F., 2012. Age and magmatic evolution
685 of the Famatinian granitic rocks of Sierra de Ancasti, Sierras Pampeanas, NW Argentina.
686 Journal of South American Earth Sciences 34, 10-25.

687 Dare, S.A.S., Pearce, J.A., McDonald, I., Styles, M.T., 2009. Tectonic discrimination of
688 peridotites using fO_2–Cr# and Ga–Ti–Fe^{III} systematics in chrome–spinel. Chemical
689 Geology 261 (3–4), 199-216.

690 Davis, J., Roeske, S.M., McClelland, W.C., Kay, S.M., 2000. Mafic and ultramafic crustal
691 fragments of the southwestern Precordillera terrane and their bearing on tectonic models of
692 the early Paleozoic in western Argentina. Geology 28, 171–174.

693 Díaz, L., Vivallo, W., Alfaro, G. & Cisternas M. E. 1988. Geoquímica de los esquistos
694 paleozoicos de Bahia Mansa, Osorno, Chile. In: Congreso Geológico Chileno No. 5,
695 Actas, E75-E96. Santiago, Chile.

696 Escayola, M., Proenza, J.A., Schalamuk, A., Cábana, C., 2004. La secuencia ofiolítica de la
697 faja ultramáfica de Sierras Pampeanas de Córdoba, Argentina. In: Pereira, E., Castroviejo,
698 R., Ortiz, F. (Eds.), Complejos ofiolíticos en Iberoamérica, Proyecto XIII.1— CYTED, pp.
699 133–155.

700 Forsythe, R., 1982. The late Paleozoic and Early Mesozoic evolution of southern South
701 America: A plate tectonic interpretation. Journal of the Geological Society of London,
702 139, 671–682.

703 Frei, R., Gervilla, F., Meibom, A., Proenza, J.A., Garrido, C.J., 2006. Os isotope
704 heterogeneity of the upper mantle: evidence from the Mayarí–Baracoa ophiolite belt in
705 eastern Cuba. Earth and Planetary Science Letters 241, 466–476.

706 Frutos, J., Alfaro, G., 1987. Metallogenic and tectonic characteristics of the Paleozoic
707 ophiolitic belt of the southern Chile Coastal Cordillera. Geologische Rundschau, 76, 343-
708 356.

709 Galdames, C., Rabbia, O.M., Alfaro, G., Hernández, L., 2011. Platinum-Group Elements in
710 Ultramafic Rocks from La Cabaña Area, Coastal Cordillera of South-Central Chile. 11th
711 International Platinum Symposium. Ontario Geological Survey, Miscellaneous Release–
712 Data 269.

713 Garuti, G., Zaccarini, F., Moloshag, V., Alimov, V., 1999. Platinum-group elements as
714 indicators of sulphur fugacity in ophiolitic upper mantle: an example from chromitites of
715 the Ray-Iz ultramafic complex, Polar Urals, Russia. The Canadian Mineralogist 37, 1099–
716 1115.

717 Garuti, G., Puskarev, E.V., Zaccarini, F., Cabella, R., Anikina, E.V., 2003. Chromite
718 composition and platinum-group mineral assemblage in the Uktus Alaskan type complex
719 (central Urals, Russia). Mineralium Deposita 38, 312–326.

720 Garuti, G., Pushkarev, E., Zaccarini, F., 2005. Diversity of chromite-PGE mineralization in
721 ultramafic complexes of the Urals. In: Törmänen, T.O., Alapieti, T.T. (Eds.), Platinum-
722 group elements—from genesis to beneficiation and environmental impact. Tenth Int.
723 Platinum Symposium (Oulu), pp. 341–344.

724 Gervilla, F., Proenza, J.A., Frei, R., González-Jiménez, J.M., Garrido, C.J., Melgarejo, J.C.,
725 Meibom, A., Díaz-martínez, R., Lavaut, W., 2005. Distribution of platinum-group
726 elements and Os isotopes in chromite ores fromMayarí–Baracoa Ophiolilte Belt (eastern
727 Cuba). Contributions to Mineralogy and Petrology 150, 589–607.

728 Gervilla, F., Padrón-Navarta, J.A., Kerestedjian, T., Sergeeva, I., González-Jiménez, J.M.,
729 Fanlo, I., 2012. Formation of ferrian chromite in podiform chromitites from the Golyamo
730 Kamenyane serpentinte, Eastern Rhodopes, SE Bulgaria: a two-stage process.
731 Contributions to Mineralogy and Petrology. http://dx.doi.org/10.1007/s00410-012-0763-3.

732 Ghosh, B., Pal, T., Bhattacharya, A., Das, D., 2009. Petrogenetic implications of ophiolitic
733 chromite from Rutland Island, Andaman—a boninitic parentage in supra-subduction
734 setting. Mineralogy and Petrology 96, 59-70. DOI: DOI 10.1007/s00710-008-0039-9.

735 Glodny, J., Lohrmann, J., Echtler, H., Gräfe, K., Seifert, W., Collao, S., Figueroa, O. 2005.
736 Internal dynamics of a paleoaccretionary wedge: insights from combined isotope
737 tectonochronology and sandbox modelling of the south-central Chilean forearc. Earth and
738 Planetary Science Letters, 231, 23–39.

739 Glodny, J., Echtler, H., Collao, S., Ardiles, M., Burón, P., Figueroa, O., 2008. Differential
740 Late Paleozoic active margin evolution in South-Central Chile (37°S–40°S) – the
741 Lanalhue Fault Zone. Journal of South American Earth Sciences, 26, 397-411

742 Godoy, E., Kato, T. 1990. Late Palaeozoic serpentinites and mafic schists from the Coast
743 Range accretionary complex, central Chile: their relation to aeromagnetic anomalies.
744 Geologische Rundschau, 79, 121–130.

745 González-Jiménez, J.M., Proenza, J.A., Gervilla, F.,Melgarejo, J.C., Blanco-Moreno, J.A.,
746 Ruiz- Sánchez, R., Griffin, W.L., 2011. High-Cr and high-Al chromitites from the Sagua
747 de Tánamo district, Mayarí-Cristal Ophiolitic Massif (eastern Cuba): constraints on their
748 origin from mineralogy and geochemistry of chromian spinel and platinum-group
749 elements. Lithos 125, 101–121.

750 González-Jiménez, J.M., Gervilla, F., Griffin, W.L., Proenza, J.A., Augé, T., O'Reilly, S.Y.,
751 Pearson, N.J., 2012a. Os-isotope variability within sulfides frompodiformchromitites.
752 Chemical Geology 291, 224–235.

753 González-Jiménez, J.M., Griffin, W.L., Gervilla, F., Kerestedjian, T.N., O'Reilly, S.Y.,
754 Proenza, J.A., Pearson, N.J., Sergeeva, I., 2012b. Metamorphismdisturbs the Re–Os
755 signatures of platinum-group minerals in ophiolite chromitites. Geology.
756 http://dx.doi.org/10.1130/G33064.1.

757 González-Jiménez, J.M., Marchesi, C., Griffin, W.L., Gutiérrez-Narbona, R., Lorand, Jean.-P,
758 O'Reilly, S.Y., Garrido, C.J., Gervilla, F., Pearson, N.J., Hidas, K., 2013a. Transfer of Os
759 isotopic signatures from peridotite to chromitite in the subcontinental mantle: insights
760 from in situ analysis of platinum-group and base-metal minerals (Ojén peridotite massif,
761 southern Spain). Lithos. http://dx.doi.org/10.1016/j.lithos.2012.07.009.

762 González-Jiménez, J.M., Griffin, W.L., Gervilla, F., Proenza, J.A., O'Reilly, S.Y., Pearson,
763 N.J., 2013b. Chromitites in ophiolites: How, where, when, why? Part I. A review and new
764 ideas on the origin and significance of platinum-group minerals. Lithos 189, 127-139.

765 González-Jiménez, J.M., Griffin, W.L., Proenza, J.A., Gervilla, F., O'Reilly, S.Y., Akbulut,
766 M., Pearson, N.J., Arai, S., 2013c. Chromitites in ophiolites: How, where, when, why?
767 Part II. The crystallization of chromitites. Lithos.
768 http://dx.doi.org/10.1016/j.lithos.2013.09.008.

769 González-Jiménez, J.M., Locmelis, M., Belousova, E., Griffin, W.L., Gervilla, F.,
770 Kerestedjian, T.N., Pearson, N.J., Sergeeva, I., 2013d. Genesis and tectonic implications
771 of podiform chromitites in the metamorphosed Ultramafic Massif of Dobromirtsi
772 (Bulgaria). Gondwana Res. DOI: http://dx.doi.org/10.1016/j.gr.2013.09.020.

773 Graham, I.T., Franklin, B.J., Marshall, B., 1996. Chemistry and mineralogy of podiform
774 chromitite deposits, southern NSW, Australia: a guide to their origin and evolution.
775 Mineralogy and Petrology 37, 129–150.

776 Griffin,W.L., O'Reilly, S.Y., Afonso, J.C., Begg, G.C., 2009. The composition and evolution
777 of Lithospheric mantle: a re-evaluation and its tectonic implications. Journal of Petrology
778 50 (7), 1185–1204. http://dx.doi.org/10.1093/petrology/egn033.

779 Hervé, F. 1974. Petrology of the crystalline basement Nahuelbuta Mountains, South-Central
780 Chile. PhD thesis, Hokkaido University.

781 Hervé, F. 1977. Petrology of the Crystalline Basement of the Nahuelbuta Mountains,
782 Southcentral Chile. *In*: ISHIKAWA, T. & AGUIRRE, L. (eds) *Comparative Studies on the*
783 *Geology of the Circum Pacific Orogenic Belt in Japan and Chile*. Japan Society for the
784 Promotion of Science, Tokyo, 1–51.

785 Hervé, F., Davidson, J., Godoy, E., Mpodozis, C., Covacevich, V. 1981. The Late Paleozoic
786 in Chile: stratigraphy, structure and possible tectonic framework. Revista da Academia do
787 Ciencias Brasil, 53, 361–373.

788 Hervé, F., Godoy, E., Parada, M. A., Ramos, V., Rapela, C., Mpodozis, C., Davidson, J. A.
789 1987. A general view of the Chilean-Argentine Andes, with emphasis on their early

790 history. In: MONGER, J. W. H. & FRANCHETEAU, J. (eds.) Circum-Pacific Orogenic
791 Belts and the Evolution of the Pacific Ocean Basin. Geodynamics Series 18, 97–113.

792 Hervé, F., Munizaga, F., Parada, M. A., Brook, M., Pankhurst, R., Snelling, N., Drake, R.
793 1988. Granitoids of the Coast Range of central Chile: Geochronology and geological
794 setting. Journal of South American Earth Sciences, 1, 185–195.

795 Hervé, F., Calderón, M., Fanning, C. M., Pankhurst, R. J., Godoy, E. 2012. Provenance
796 variations in the Late Paleozoic accretionary complex of central Chile as indicated by
797 detrital zircons. Gondwana Research, 23, 1122-1135

798 Hicky, R.L., Frey, F.A., 1982. Geochemical characteristics of boninite serives volcanic:
799 implication for their source. Geochimica et Cosmochimica Acta 46, 2099-2115.

800 Höfer, C., Kraus, S., Miller, H., Alfaro, G., Barra, F., 2001. Chromite-bearing serpentinite
801 bodies within an arc-backarc metamorphic complex near La Cabana, south Chilean
802 Coastal Cordillera. Journal of South American Earth Sciences 14, 113–126.

803 Hufmann, L., Massonne, H. 2000. Ancient arc/back-arc and N-MORB volcanics incorporated
804 in the Late Palaeozoic/Early Mesozoic metamorphic complex of the Coastal Cordillera of
805 Chiloé, Southern Central Chile. In Congreso Geológico Chileno, No. 9, Actas 2, 738-741.
806 Puerto Varas, Chile.

807 Jugo, P., 2009. Sulfur content at sulfide saturation in oxidized magmas. Geology 37, 415-
808 418.

809 Kamenetsky, V.S., Crawford, A.J., Meffre, S., 2001. Factors controlling chemistry of
810 magmatic spinel: an empirical study of associated olivine, Cr-spinel and melt inclusions
811 from primitive rocks. Journal of Petrology 42, 655–671.

812 Keppie, J.D., Ramos, V.A., 1999. Odyssey of terranes in the Iapetus and Rheic oceans during
813 the Paleozoic. In: Ramos, V.A., Keppie, J.D. (eds.), Laurentia–Gondwana connections
814 before Pangea: Geological Society of America Special Paper, 336, 267–276.

815 Kocks, H., Melcher, F., Meisel, T., Burgath, K.P., 2007. Diverse contributing sources to
816 chromitite petrogenesis in the Shebenik Ophiolitic Complex, Albania: evidencefrom new
817 PGE and Os-isotope data. Mineralogy and Petrology 91, 139–170.

818 Leblanc, M., Nicolas, A., 1992, Les chromitites ophiolitiques: Chronique de la Recherche
819 Minière, 507, p. 3−25.

820 Leblanc, M., 1986., Chromite in ocean arc environments: New Caledonia. In: Stowe CW (ed)
821 Evolution of chromium ore fields. Van Nostrand Rheinhold, New York, pp 265-296.

822 Liu, C.Z., Snow, J.E., Brügmann, G., Hellebrand, E., Hofmann, A.W., 2009. Non-chondritic
823 HSE budget on Earth's upper mantle evidenced by abyssal peridotites from Gakkel ridge
824 (Artic Ocean). Earth and Planetary Science Letters 283, 122-132.

825 Lucassen, F., Trumbull, R., Franz, G., Creixell, C., VásqueZ, P., Romer, R. L., Figueroa, O.
826 2004. Distinguishing crustal recycling and juvenile additions at active continental margins:
827 the Paleozoic to recent compositional evolution of the Chilean Pacific margin (36–41°S).
828 Journal of South American Earth Sciences, 17, 103–119.

829 Malitch, K.N., 2004. Osmium isotope constraints on contrasting sources and prolonged
830 melting in the Proterozoic upper mantle: evidence from ophiolitic Ru–Os sulfides and Ru–
831 Os–Ir alloys. Chemical Geology 208, 157–173.

832 Malitch, K.N., Junk, S.A., Thalhammer, O.A.R., Melcher, F., Knauf, V.V., Pernicka, E.,
833 Stumpfl,E.F., 2003. Laurite and ruarsite from podiformchromitites at Kraubath and
834 Hochgrössen, Austria: new insights from osmium isotopes. The Canadian Mineralogist 41,
835 331–352.

836 Malpas, J., Robinson, P.T., Zhou, M.-F., 1997. Chromite and ultramafic rock compositional
837 zoning through a paleotransform fault, Poum, New Caledonia: discussion. Economic
838 Geology 92, 502–503.

839 Marchesi, C., González-Jiménez, J.M., Gervilla, F., Garrido, C.J., Griffin, W.L., O'Reilly,
840 S.Y., Proenza, J.A., Pearson, N.J., 2011. In situ Re–Os isotopic analysis of platinum-group
841 minerals from the Mayarí–Cristal ophiolitic massif (Mayarí–Baracoa Ophiolitic Belt,
842 eastern Cuba): implications for the origin of Os-isotope heterogeneities in podiform
843 chromitites. Contributions to Mineralogy and Petrology 161, 977–990.

844 Maurel, C., Maurel, P., 1982. Étude expérimentale de la distribution de l´aluminium entre
845 bain silicaté basique et spinelle chromifère. Implications pétrogénétiques : teneur en
846 chrome des spinelles. Bulletin de Minéralogie. 105, 197-202.

847 Melcher, F., Grum, W., Simon, G., Thalhammer, T.V., Stumpfl, E.F., 1997. Petrogenesis of
848 the ophiolitic giant chromite deposits of Kempirsai, Kazakhstan: a study of solid and fluid
849 inclusions in chromite. Journal of Petrology 38, 1419–1458.

850 Meisel, T., Walker, R.J., Morgan., 1996. The osmium isotopic composition of the Earth's
851 primitive upper mantle. Nature 383, 517-520.

852 Meisel, T., Melcher, F., 2004. A metamorphosed Early Cambrian Crust-Mantle Transition in
853 the Easterh Alps-Austria. Journal of Petrology 45, 1689-1723.

Mpodozis, C., Kay, S. M., 1990. Provincias magmáticas ácidas y evolución tectónica de Gondwana: Andes chilenos (28–31°S). Revista Geológica de Chile, 17, 153–180.

Mpodozis, C., Kay, S. M. 1992. Late Paleozoic to Triassic evolution of the Gondwana margin: evidence from Chilean Frontal Cordilleran batholiths (28ºS to 31ºS). Geological Society of America Bulletin, 104, 999–1014.

Naldrett, A., Duke, J.M., 1980. Ptmetlas inmagmatic sulfide ores. Sciences 208, 1417–1424.

Naldrett, A.J., Wilson, A., Kinnaird, J., Yudovskaya, M., Chunnett, G., 2011. The origin of chromitites and related PGE mineralization in the Bushveld Complex: new mineralogical and petrological constraints. Mineralium Deposita 47 (3), 209–232.

O'Driscoll, B., Day, J.M.D., Walker, R.J., Daly, J.S., McDonough, W. F., Piccoli, P.M., 2012. Chemical heterogeneity in the upper mantle recorded by peridotites and chromitites from the Shetland Ophiolite Complex, Scotland. Earth and Planetary Science Letters 333-334, 226-237.

O'Reilly, S.Y., Zhang, M., Griffin, W.L., Begg, G., Hronsky, J., 2009. Ultradeep continental roots and their oceanic remnants: a solution to the geochemical "mantle reservoir"problem? Lithos 112 (2), 1043–1054.

Pagé, P., Barnes, S.-J., 2009. Using trace elements in chromites to constrain the origin of podiform chromitites in the Thetford Mines ophiolite, Québec, Canada. Economic Geology 104, 997–1018.

Prichard, H.M., Neary, C.R., Fisher, F.C., O'Hara, M.J., 2008. PGE-rich Podiform chromitites in the Al'Ays ophiolite complex, Saudi Arabia: an example of critical mantle melting to extract and concentrate PGE. Economic Geology 103, 1507–1529.

Proenza, J.A., Gervilla, F., Melgarejo, J.C., Bodinier, J.L., 1999. Al- and Cr-rich chromitites from the Mayarí–Baracoa Ophiolitic Belt (Eastern Cuba): consequence of interaction between volatile-rich melts and peridotites in suprasubduction mantle. Economic Geology 94, 547–566.

Proenza JA, Ortega-Gutiérrez, F., Camprubí, A., Tritlla, J., Elías-Herrera, M., Reyes-Salas, M., 2004. Paleozoic serpentinite-enclosed chromitites from Tehuitzingo (Acatlan complex, southern Mexico): a petrological and mineralogical study. Journal of South American Earth Sciences 16, 649–666.

Proenza, J.A., Zaccarini, F., Lewis, J.F., Longo, F., Garuti, G., 2007. Chromian spinel composition and the platinum-group minerals of the PGE-rich Loma Peguera chromitites, Loma Caribe peridotite, Dominican Republic. The Canadian Mineralogist 45, 631–648.

887 Proenza, J.A., Zaccarini, F., Escayola, M., Cábana, C., Shalamuk, A., Garuti, G., 2008.
888 Composition and textures of chromite and platinum-group minerals in chromitites of the
889 western ophiolitic belt from Córdoba Pampeans Ranges, Argentine. Ore Geology Reviews
890 33, 32–48.

891 Rabbia, O.M., Alfaro, G., Barra, F. 1994. Presencia de espilitas metasomatizadas en el
892 cinturón serpentinítico de la Cordillera de la Costa del sur de Chile. II Jornadas de
893 Mineralogía, Petrografía y Metalogénesis de Rocas Ultrabásicas. Universidad Nacional de
894 La Plata, Argentina, 3, 607-615.

895 Ramos, V. A. 2008. The Basement of the Central Andes: The Arequipa and Related Terranes.
896 Annua Review of Earth and Planetary Sciences, 36, 289-324

897 Ramos, V.A. 2009. Anatomy and global context of the Andes: Main geologic features and the
898 Andean orogenic cycle. The Geologica society of America Memoir 204, 31-65.

899 Ramos, V.A., Basei, M., 1997. The basement of Chilenia: an exotic continental terrane to
900 Gondwana during the Early Paleozoic. Terrane Dynamics 97, International Conference on
901 Terrane Geology, Christchurch, New Zealand, conference abstracts, 140–143

902 Ramos V.A., Jordan T., Allmendinger R.W., Kay S.M., Cortes J.M. & Palma M.A. 1984.
903 Chilenia un terreno alóctono en la evolución paleozoica de los Andes Centrales.
904 In: Congreso Geológico Argentino No 9, Actas, 2, 84–106.

905 Ramos, V. A., Jordan, T. E., Allmendinger, R. W., Mpodozis, C., Kay, S. M., Cortés, J. M.,
906 Palma, 1986. Paleozoic terranes of the Central Argentine – Chilean Andes. Tectonics, 5,
907 855–880.

908 Ramos, V., Vujovicha, G., Martino, R., Otamendi, J., 2010. Pampia: A large cratonic block
909 missing in the Rodinia supercontinent. Journal of Geodynamics 50, 243–255.

910 Rapalini, A. E., Vilas, J. F. 1991. Tectonic rotations in hte Late Palaeozoic continental margin
911 of southern South America determined and dated by paleomagnetism. Geophysical Journal
912 International, 107, 333-351

913 Roberts, S., 1988. Ophiolitic chromitite formation: A marginal basin phenomenon? Economic
914 Geology 83, 1034–1036.

915 Robinson, P., Adetunji. J., 2013. The geochemistry and oxidation state of podiform
916 chromitites from the mantle section of the Oman ophiolite: a review. Gondwana Research.
917 DOI: http://dx.doi.org/10.1016/j.gr.2013.07.013

918 Rollinson, H.R., 2005. Chromite in the mantle section of the Oman ophiolite: a new genetic
919 model. Island Arc 14:542–550

920 Rollinson, H., 2008. The geochemistry of mantle chromitite from the northern part of the
921 Oman ophiolite: inferred parental melt compositions. Contributions to Mineralogy and
922 Petrology 156, 273–288.

923 Schira, W., Amstutza, GG.C., Fontboté, L. The Pirpen Alto Cu-(Zn) Massive Sulfide
924 Occurrence in South-Central Chile – A Kieslager-Type Mineranlization in a Paleozoic
925 Ensialic Mature Marginal Basin Setting. In: FONTBOTË, L., AMSTUTZ, G. C.,
926 CARDOZO, M., CEDILLO, E. & FRUTOS, J. (eds) Stratabound Ore Deposits in the
927 Andes. Springer, Berlin, 229-251.

928 Shi, R., Alard, O., Zhi, X., O'Reilly, S.Y., Pearson, N.J., Griffin,W.L., Zhang, M., Chen, X.,
929 2007. Multiple events in the Neo-Tethyan oceanic upper mantle: evidence from Ru–Os–Ir
930 alloys in the Luobusa and Dongqiao ophiolitic podiform chromitites, Tibet. Earth and
931 Planetary Science Letters 261, 33–48.

932 Shi, R., Griffin, W.L., O'Reilly, S.Y., Zhou, M.F., Zhao, G., Huang, Q., Zhang, X., Ding,
933 D.L., 2012. Archean Mantle contributes to the genesis of chromitites in the Paleozoic
934 Sartohay ophiolite, Asiatic Orogenic Belt, northwestern China. Precambrian Research
935 216-219, 87-94.

936 Shirey, S.B., Walker, R.J., 1995. Re-Os isotopes in cosmochemistry and high-temperature
937 geochemistry. Annual Review of Earth and Planetary Science 26, 423-500.

938 Snow, J., Reisberg, L., 1995. Os isotopic systematics of the MORB mantle: results from
939 altered abyssal peridotites. Earth and Planetary Science Letters 133, 411-421.

940 Tang, Y.-J., Zhang, H.-F., Ying, J.-F., Su, B.-X., 2013. Widespread refertilization of cratonic
941 and circum-cratonic lithospheric mantle. Earth Science Reviews 118, 45–68.

942 Tsuru, A., Walker, R.J., Kontinen, A., Peltonen, P., 2000. Re–Os isotopic systematics of the
943 1.95 Ga Jormua Ophiolite Complex, northeastern Finland. Chemical Geology

944 164, 123–141.

945 Uysal, I., Tarkian, M., Sadiklar, M.B., Zaccarini, F., Meisel, T., Garuti, G., Heidrich, S.,
946 2009. Petrology of Al- and Cr-rich ophiolitic chromitites from the Muğla, SW Turkey:
947 implications from composition of chromite, solid inclusions of platinum-group mineral,
948 silicate, and base-metal mineral, and Os-isotope geochemistry.Contributions to
949 Mineralogy and Petrology 158, 659–674.

950 Vatin-Perignon, N., Amossé, J., Radelli, L., Keller, F., Castro-Leyva, T., 2000. Platinum
951 group element behaviour and thermochemical constraints in the ultrabasic–basic complex
952 of the Vizcaino Peninsula, Baja California Sur, Mexico. Lithos, 53, 59-80.

953 Vergara, L. 1970. Prospección de yacimientos de cromo y hierro en La Cabaña, Cautín.
954 Bachelor´s thesis. Universidad de Chile. 96 pp.

955 Vivallo, W., Alfaro, G., Diaz, L. 1988. Las metabasaltos de la Serie Occidental de la
956 Cordillera de la Costa entre los 38°-41°S latitud Sur, Chile: evidencias geoquímicas de
957 cuenca marginal durante el Paleozoico. VII Congresso Latinoamericano de Geología
958 (Belém), Actas, 1, 260-273.

959 Walker, R.J., Horan, M.F., Morgan, J.W., Becker, H., Grossman, J.N., Rubin, A.E., 2002a.
960 Comparative ^{187}Re–^{187}Os systematics of chondrites: implications regarding early solar
961 system processes. Geochimica et Cosmochimica Acta 66, 4187–4201.

962 Walker, R.J., Prichard, H.M., Ishiwatari, A., Pimentel, M., 2002b. The osmium isotopic
963 composition of convecting upper mantle deduced from ophiolite chromites. Geochimica et
964 Cosmochimica Acta 66, 329–345.

965 Wasylenki, L.E., Baker, M.B., Kent, A.J.R., Stolper, E.M., 2003. Nearsolidus melting of the
966 shallow upper mantle: partial melting experiments on depleted peridotite. Journal of
967 Petrology 44, 1163–1191

968 Willner, A. P., Hervé, F., Massonne, H.-J., 2000. Mineral chemistry and pressure–
969 temperature evolution of two contrasting highpressure–low-temperature belts in the
970 Chonos Archipelago, Southern Chile. Journal of Petrology 41, 309–330.

971 Willner, A. P. 2005. Pressure-temperature evolution of an Upper Paleozoic paired
972 metamorphic belt in Central Chile (34°–35°30´S). Journal of Petrology, 46, 1805–1833.

973 Willner, A. P., Thomson, S. N., Kröner, A., Wartho, J., Wijbrans, J. R., Hervé, F. 2005. Time
974 markers for the evolution and exhumation history of a Late Paleozoic paired metamorphic
975 belt in north-central Chile (34°–35°30pS). Journal of Petrology, 46, 1835–1858.

976 Zaccarini, F., Garuti, G., Proenza, J.A., Campos, L., Thalhammer, O.A.R., Aiglsperger,
977 T.,Lewis, J., 2011. Chromite and platinum-group-elements mineralization in the Santa
978 Elena ophiolitic ultramafic nappe (Costa Rica): geodynamic implications. Geologica Acta
979 9 (3–4), 407–423.

980 Zhou, M.F., Robinson, P.T., Malpas, J., Zijin, L., 1996. Podiform chromites in the Luobusa
981 Ophiolite (Southern Tibet): implications for melt–rock interaction and chromite
982 segregation in the upper mantle. Journal of Petrology 37, 3–21.

983 Zhou, M.F., Sun, M., Keays, R.R., Kerrich, R.W., 1998. Controls on platinum-group
984 elemental distributions of podiform chromitites of high-Cr and high-Al chromitites from
985 Chinese orogenic belt. Geochmica et Cosmochimica Acta, 677-688.

986

Table 1. Selected representative analyses of unaltered chromite at Centinela Bajo.

	011-P2–1	011-P2–9	5BF-f1–1	5BF-f1–2	5BF-f1–4	5BF-f1–5	5BF-f1–11	5BF-f1–12	5BF-f1–13	5BF-f2–31
TiO_2	0.23	0.23	0.14	0.13	0.13	0.12	0.13	0.14	0.12	0.13
Al_2O_3	17.96	18.52	17.69	17.71	17.70	17.71	17.65	17.87	18.50	17.78
V_2O_3	0.24	0.29	0.21	0.21	0.26	0.20	0.18	0.23	0.28	0.18
Cr_2O_3	50.80	48.71	51.55	51.42	51.21	51.81	51.46	51.07	51.58	51.41
Fe_2O_3	2.13	2.56	2.39	2.38	2.57	2.60	2.32	2.24	1.59	1.91
MgO	13.54	12.09	12.79	12.66	12.82	13.34	12.64	12.78	13.80	12.42
MnO	0.32	0.48	0.39	0.41	0.36	0.40	0.37	0.41	0.41	0.36
FeO	13.65	15.66	14.98	15.12	14.90	14.16	15.12	14.88	13.54	15.43
NiO	0.17	0.14	0.16	0.10	0.21	0.05	0.17	0.13	0.08	0.09
ZnO	0.02	0.13	0.05	0.10	0.05	0.21	0.05	0.03	0.02	0.10
Total	99.03	98.68	100.32	100.14	100.15	100.38	100.02	99.74	99.90	99.71
Ti	0.01	0.01	0.00	0.00	0.00	0.00	0.00	0.00	0.00	0.00
Cr	1.26	1.22	1.28	1.28	1.27	1.28	1.28	1.27	1.27	1.28
Al	0.67	0.69	0.65	0.66	0.65	0.65	0.65	0.66	0.68	0.66
V	0.00	0.00	0.00	0.00	0.00	0.00	0.00	0.00	0.00	0.00
Fe3+	0.05	0.06	0.06	0.06	0.06	0.06	0.05	0.05	0.04	0.05
Mg	0.64	0.57	0.60	0.59	0.60	0.62	0.59	0.60	0.64	0.58
Mn	0.01	0.01	0.01	0.01	0.01	0.01	0.01	0.01	0.01	0.01
Fe2+	0.36	0.42	0.39	0.40	0.39	0.37	0.40	0.39	0.35	0.41
Ni	0.00	0.00	0.00	0.00	0.01	0.00	0.00	0.00	0.00	0.00
Zn	0.00	0.00	0.00	0.00	0.00	0.00	0.00	0.00	0.00	0.00
Cr#	0.65	0.64	0.66	0.66	0.66	0.66	0.66	0.66	0.65	0.66
Mg#	0.64	0.58	0.60	0.60	0.61	0.63	0.60	0.60	0.64	0.59
Fe^{3+}#	0.12	0.13	0.13	0.12	0.13	0.14	0.12	0.12	0.10	0.10

Table 2. Platinum-group elements of chromitite samples from La Cabaña (in ppb).

	Centinela Bajo			Lavanderos		
	PODOB	CAB-7	CAB-7 B	LA-C1	LA-C2	LA-C3
Os	22	29	43	27	20	34
Ir	157	93.3	153	60.5	74.1	66
Ru	126	136	92	79	108	106
Rh	12.9	7	9.8	6.9	8.8	8.5
Pt	28	19	12	<5	13	6
Pd	<2	10	9	<2	12	3

Note: Detection limits are 5 ppb for Ru and Pt, 2 ppb for Os and Pd, 0.2 ppb for Rh, and 0.1 ppb for Ir.

Table 3. Re, Os concentration (in ppb) and Os isotopic data of selected chromite samples from the La Cabaña ultramafic bodies.

	Re	Os	$^{187}Os/^{188}Os$	$^{187}Re/^{188}Os$	$^{187}Os/^{188}O_i$	γOs	T_{MA}	T_{RD}
CEN-07	2.23	128	0.12522	0.08	0.12482	−0.13	0.33	0.32
CEN-08	0.35	202.40	0.12710	0.008	0.12706	1.66	−0.02	−0.01
CEN-09	0.20	78.69	0.12703	0.01	0.12698	1.60	0.00	0.00
LAC-1008	0.32	37.66	0.12675	0.04	0.12655	1.25	0.04	0.07

Note: The parameters to calculate the initial $^{187}Os/^{188}Os$, γOs, T_{MA}, and T_{RD} model ages and λ for $^{187}Re = 1.666 \times 10^{-11}$ a^{-1} are from Shirey and Walker (1998). Note that T_{MA} and T_{RD} model ages are expressed in Ga.

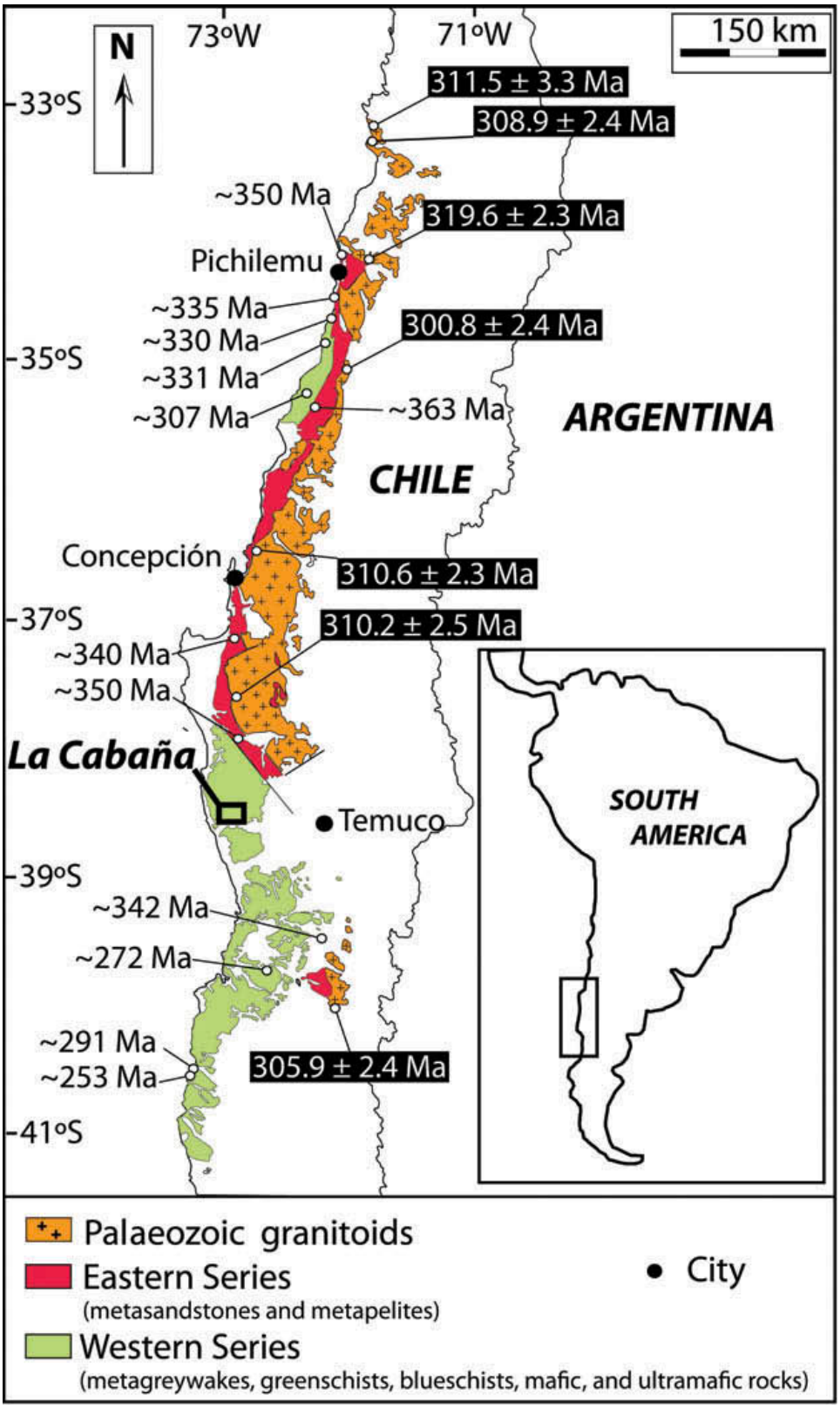
N
73°W
71°W
150 km
33°S
311.5 ± 3.3 Ma
308.9 ± 2.4 Ma
~350 Ma
319.6 ± 2.3 Ma
Pichilemu
~335 Ma
~330 Ma
~331 Ma
~307 Ma
300.8 ± 2.4 Ma
35°S
~363 Ma
ARGENTINA
CHILE
Concepción
310.6 ± 2.3 Ma
37°S
310.2 ± 2.5 Ma
~340 Ma
~350 Ma
La Cabaña
Temuco
SOUTH AMERICA
39°S
~342 Ma
~272 Ma
~291 Ma
~253 Ma
305.9 ± 2.4 Ma
41°S
Palaeozoic granitoids
Eastern Series
(metasandstones and metapelites)
Western Series
(metagreywakes, greenschists, blueschists, mafic, and ultramafic rocks)
City

Figure 1.

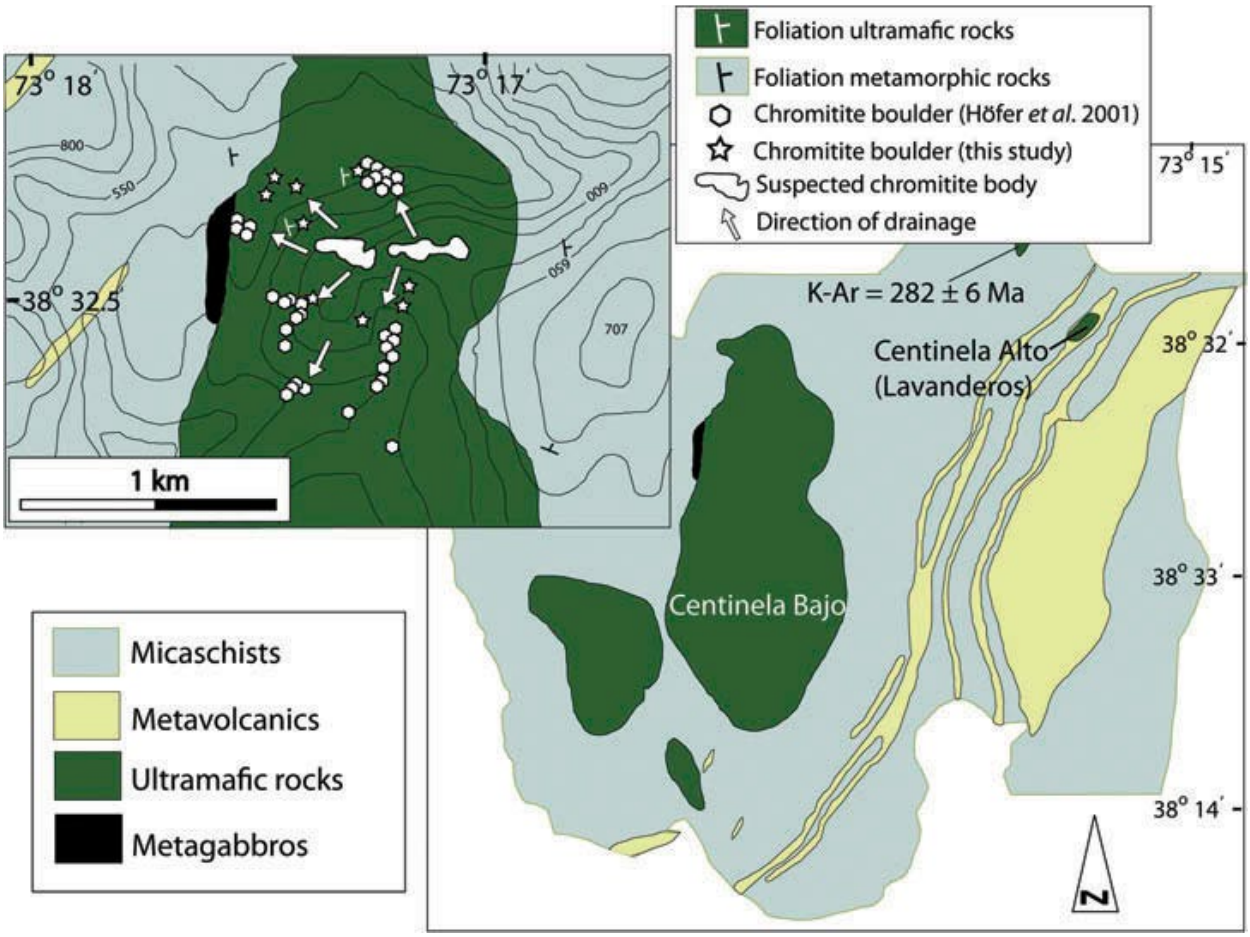
Foliation ultramafic rocks
Foliation metamorphic rocks
Chromitite boulder (Höfer et al. 2001)
Chromitite boulder (this study)
Suspected chromitite body
Direction of drainage
73° 18´
73° 17´
73° 15´
38° 32.5´
38° 32´
38° 33´
38° 14´
800
550
600
650
707
K-Ar = 282 ± 6 Ma
Centinela Alto
(Lavanderos)
Centinela Bajo
1 km
Micaschists
Metavolcanics
Ultramafic rocks
Metagabbros
N

Figure 2.

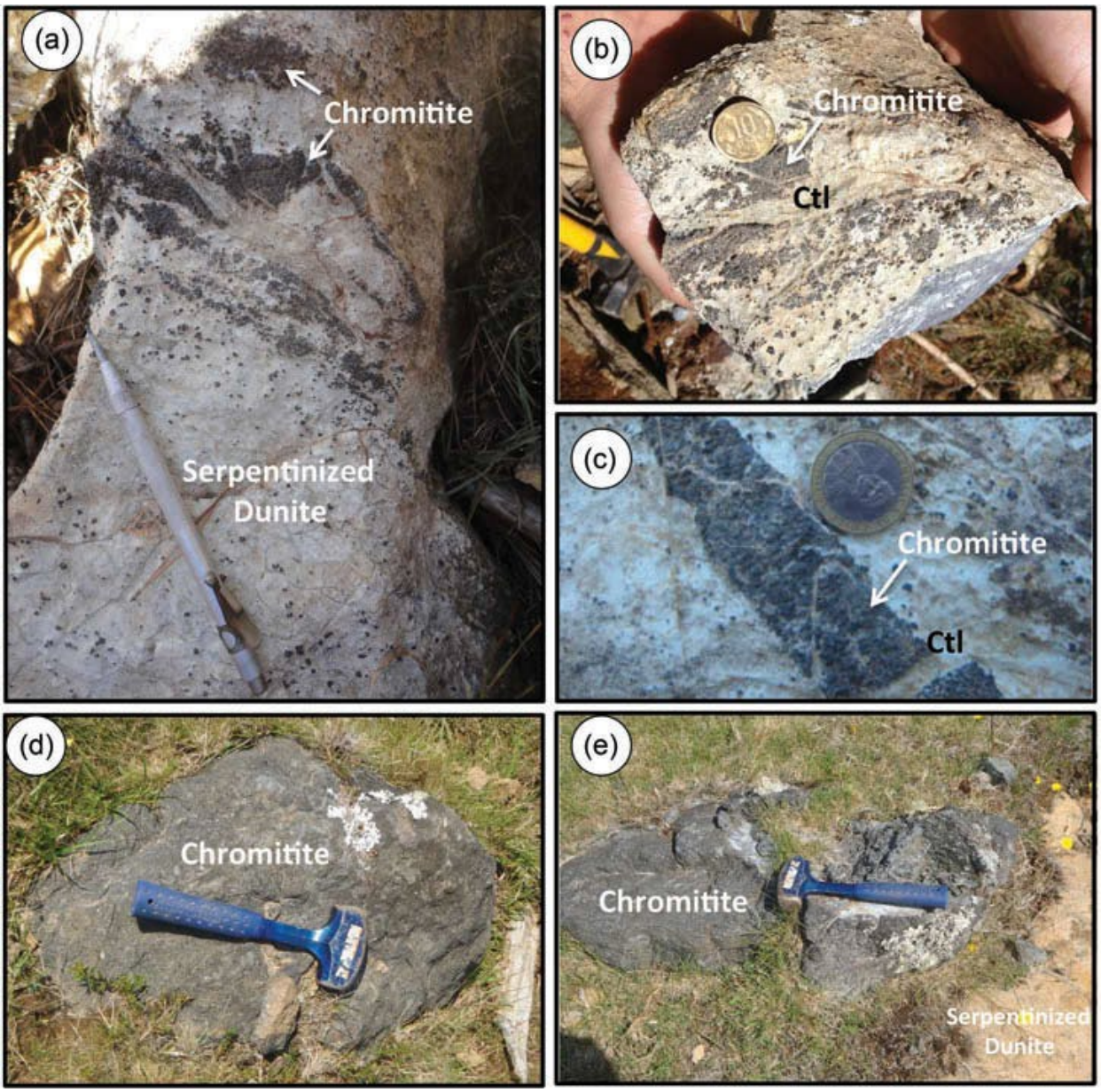
(a)
Chromitite
Serpentinized
Dunite
(b)
Chromitite
Ctl
(c)
Chromitite
Ctl
(d)
Chromitite
(e)
Chromitite
Serpentinized
Dunite

Figure 3.

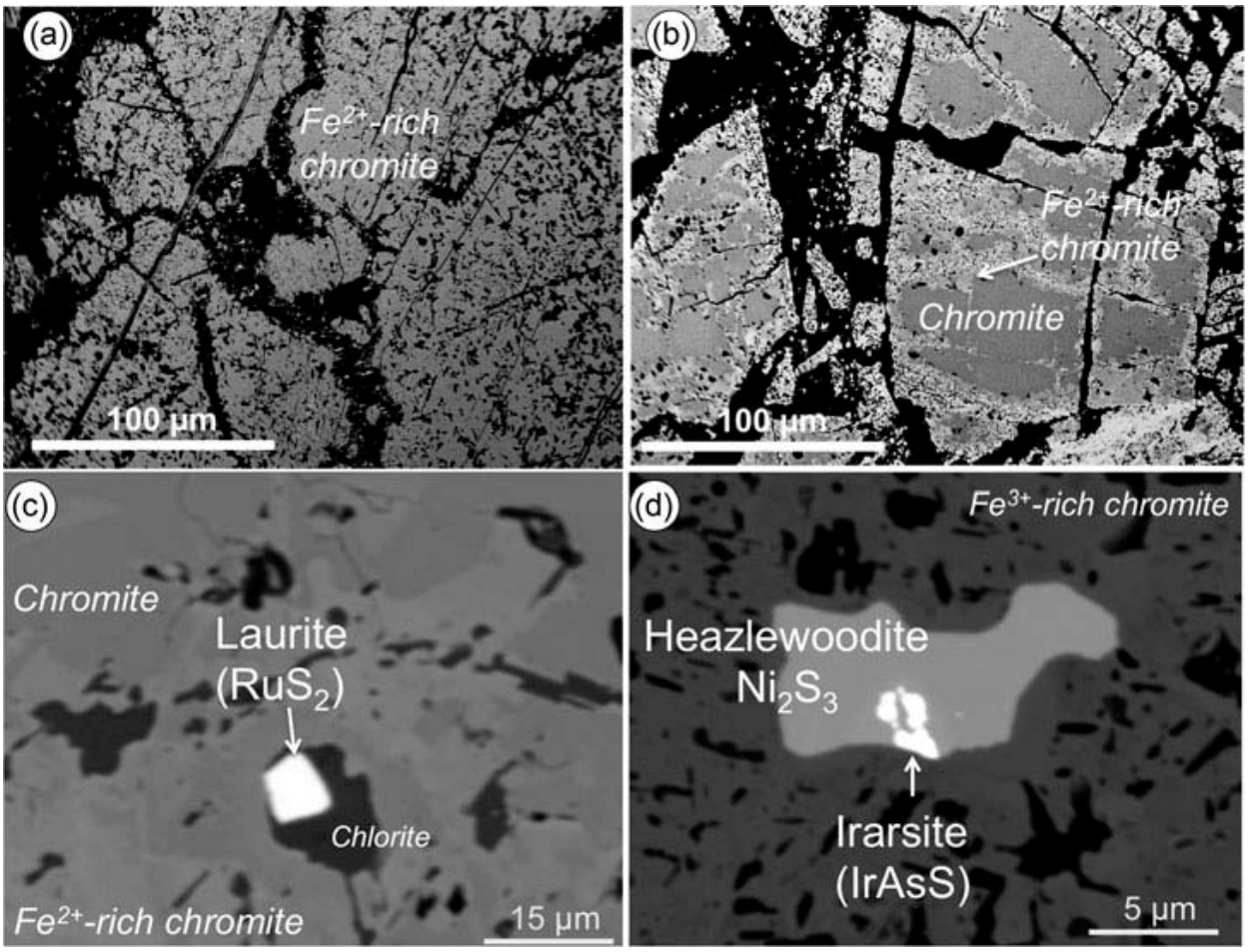
(a)
Fe2+-rich chromite
100 µm
(b)
Fe2+-rich chromite
Chromite
100 µm
(c)
Chromite
Laurite (RuS2)
Chlorite
Fe2+-rich chromite
15 µm
(d)
Fe3+-rich chromite
Heazlewoodite Ni2S3
Irarsite (IrAsS)
5 µm

Figure 4.

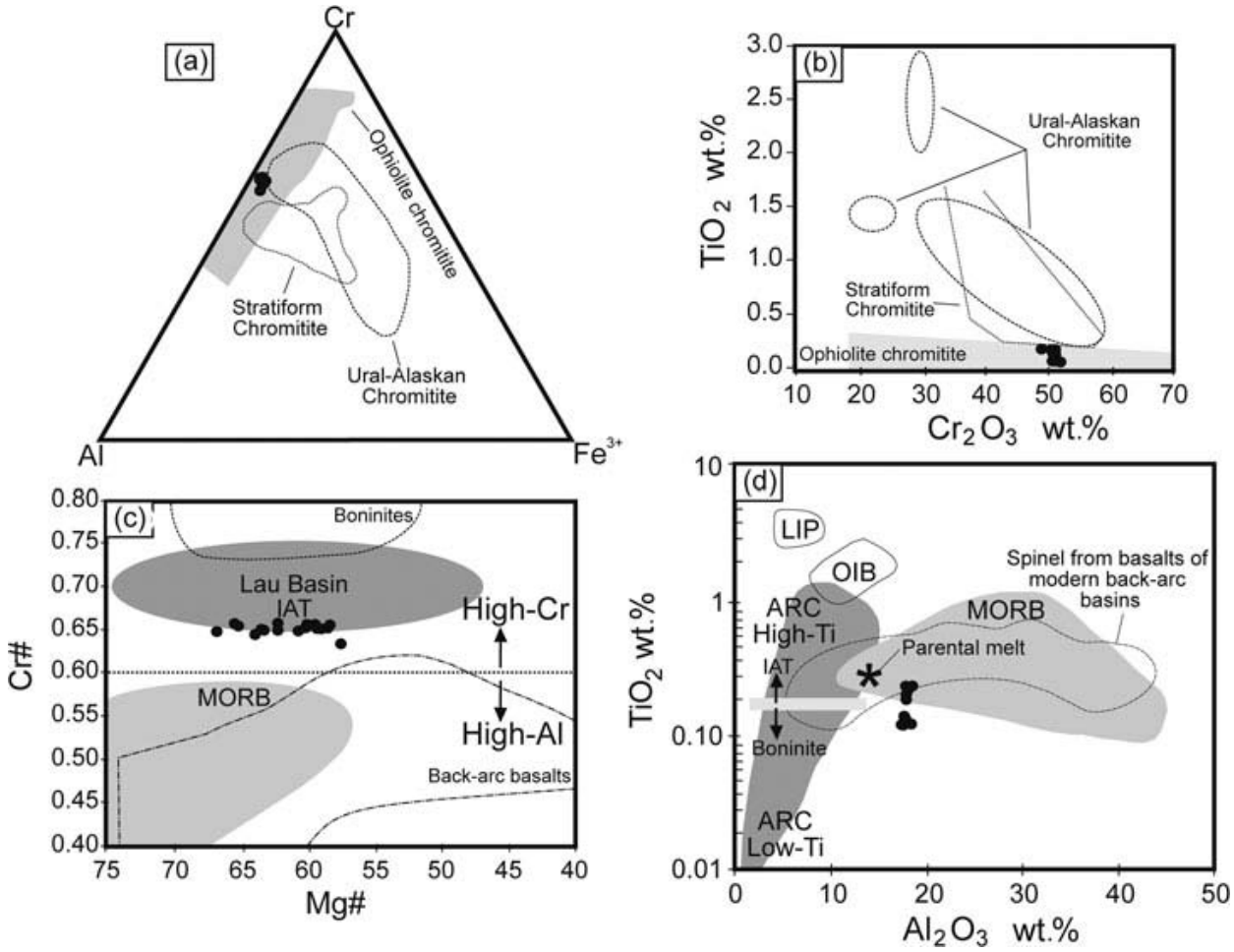
(a)
Cr
Al
Fe3+
Ophiolite chromitite
Stratiform Chromitite
Ural-Alaskan Chromitite
(b)
TiO2 wt.%
Cr2O3 wt.%
Ural-Alaskan Chromitite
Stratiform Chromitite
Ophiolite chromitite
(c)
Cr#
Mg#
Boninites
Lau Basin IAT
High-Cr
High-Al
MORB
Back-arc basalts
(d)
TiO2 wt.%
Al2O3 wt.%
LIP
OIB
ARC High-Ti
IAT
Boninite
ARC Low-Ti
MORB
Parental melt
Spinel from basalts of modern back-arc basins

Figure 5.

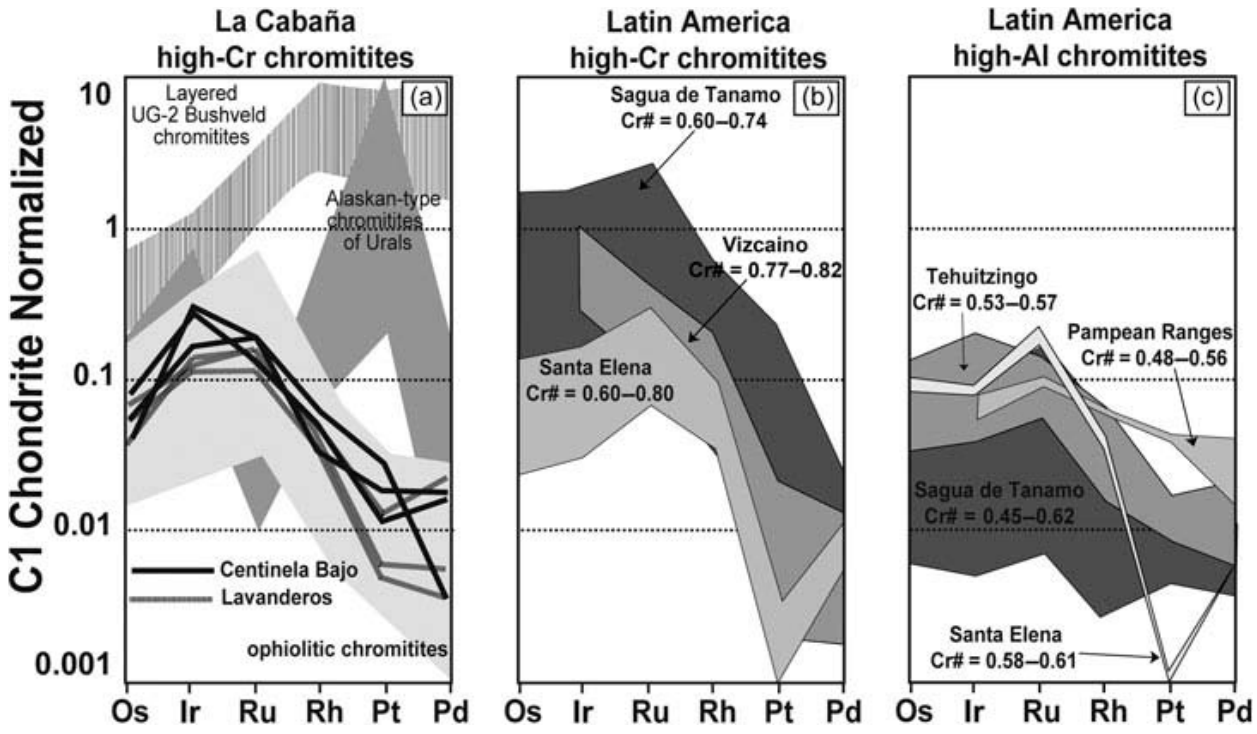

Figure 6.

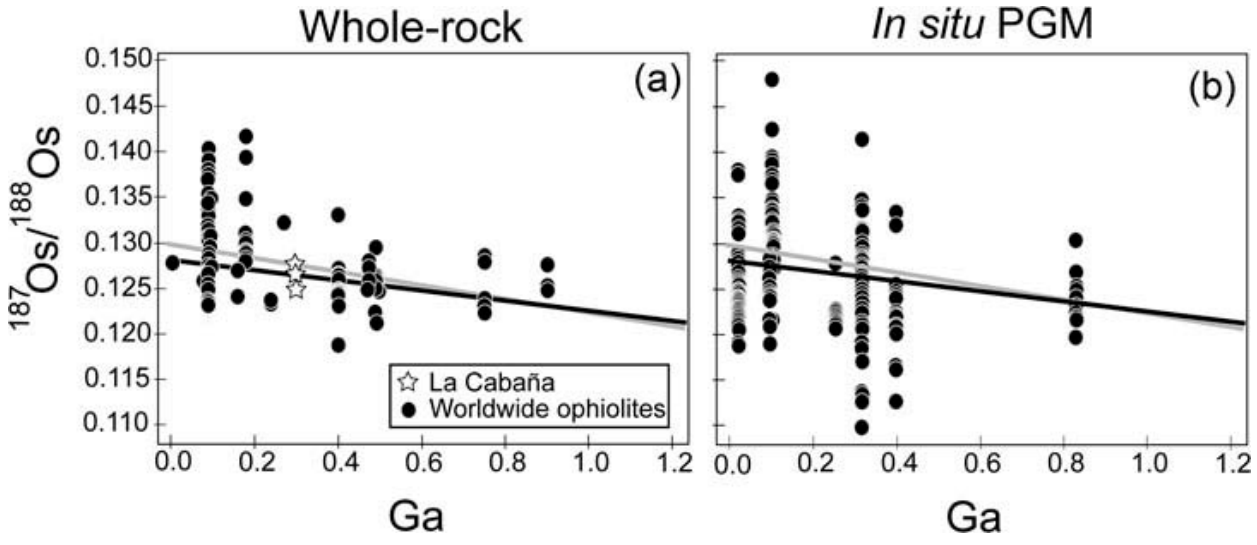

Figure 7.

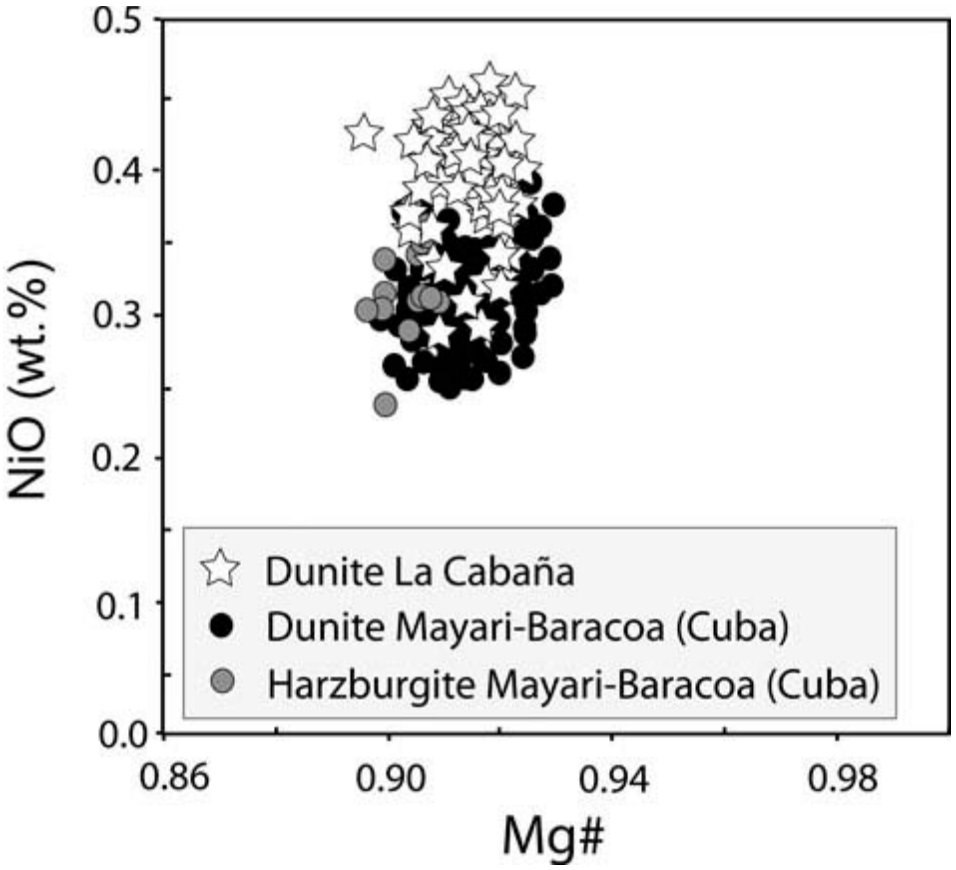
0.5
0.4
0.3
0.2
0.1
0.0
NiO (wt.%)
0.86
0.90
0.94
0.98
Mg#
Dunite La Cabaña
Dunite Mayari-Baracoa (Cuba)
Harzburgite Mayari-Baracoa (Cuba)

Figure 8.

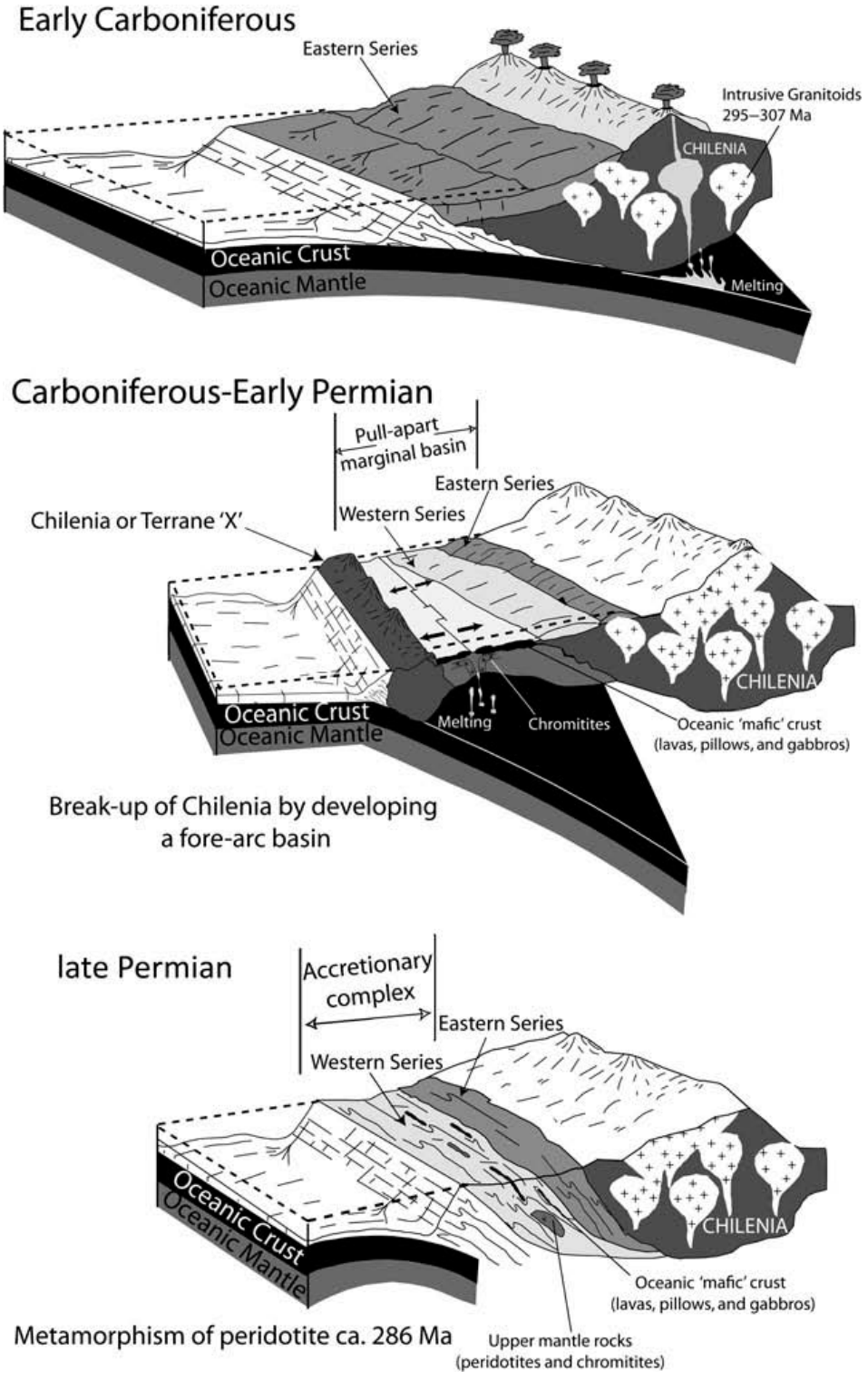
Early Carboniferous
Eastern Series
Intrusive Granitoids
295–307 Ma
CHILENIA
Oceanic Crust
Oceanic Mantle
Melting
Carboniferous-Early Permian
Pull-apart
marginal basin
Eastern Series
Western Series
Chilenia or Terrane 'X'
CHILENIA
Oceanic Crust
Oceanic Mantle
Melting
Chromitites
Oceanic 'mafic' crust
(lavas, pillows, and gabbros)
Break-up of Chilenia by developing
a fore-arc basin
late Permian
Accretionary
complex
Eastern Series
Western Series
Oceanic Crust
Oceanic Mantle
CHILENIA
Oceanic 'mafic' crust
(lavas, pillows, and gabbros)
Metamorphism of peridotite ca. 286 Ma
Upper mantle rocks
(peridotites and chromitites)

Figure 9.